Electronic Supplementary Material (ESI) for Journal of Materials Chemistry B.

Supporting Information for:

A red-emitting thiophene-modified BODIPY probe for fluorescence lifetime-based polarity imaging of lipid droplets in living cells

Rokas Žvirblis,[a,b] Karolina Maleckaitė,[a] Jelena Dodonova-Vaitkūnienė,[b] Džiugas Jurgutis,[c,d] Rugilė Žilėnaitė,[a] Vitalijus Karabanovas,[c,e] Sigitas Tumkevičius[b] and Aurimas Vyšniauskas*[a]

[a] *Center of Physical Sciences and Technology, Saulėtekio av. 3, Vilnius, LT-10257, Lithuania. E-mail: aurimas.vysniauskas@ftmc.lt*

[b] *Institute of Chemistry, Faculty of Chemistry and Geosciences, Vilnius University, Naugarduko str. 24, Vilnius, LT-03225, Lithuania*

[c] *Biomedical Physics Laboratory, National Cancer Institute, P. Baublio str. 3b, Vilnius, LT-08406, Lithuania*

[d] *Life Sciences Center, Vilnius University, Saulėtekio av. 7, Vilnius, LT-10257, Lithuania*

[e] *Department of Chemistry and Bioengineering, Vilnius Gediminas Technical University, Saulėtekio av. 11, Vilnius, LT-10223, Lithuania*

Table of Contents

1. Additional spectroscopic data

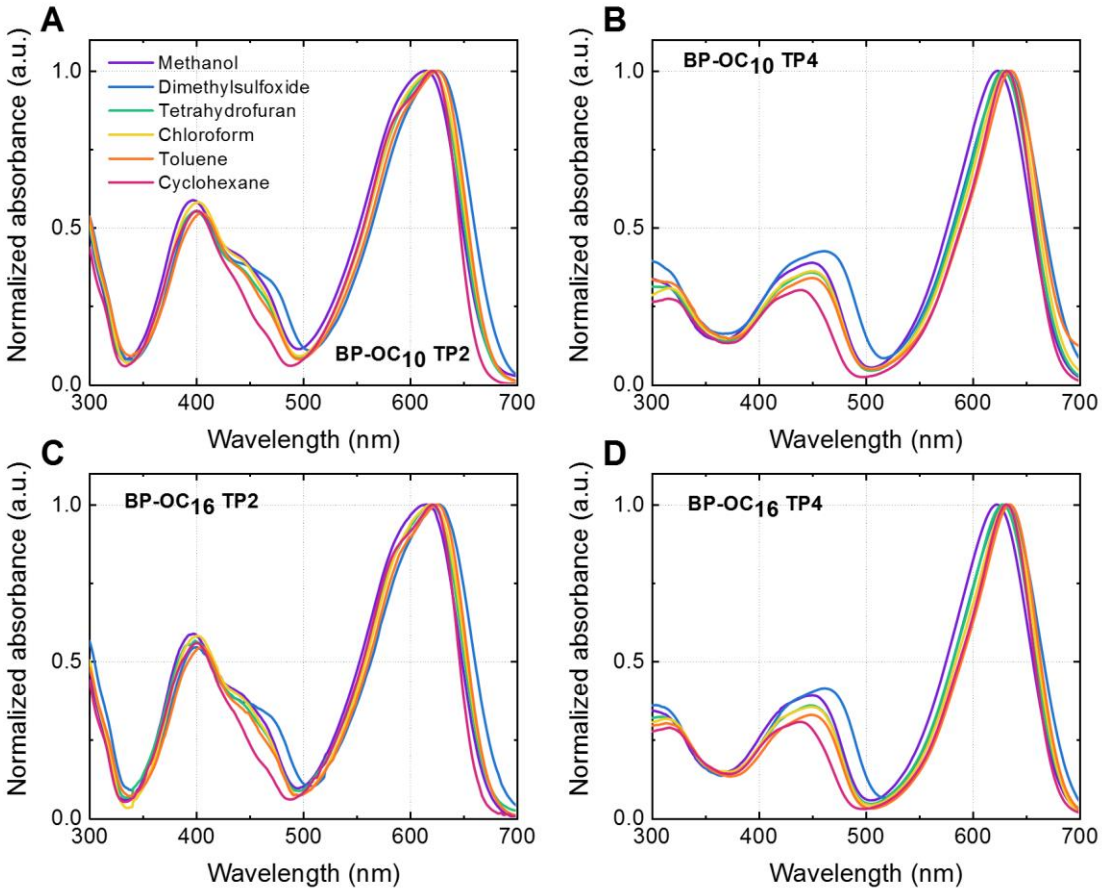

Figure S1. Normalised absorbance spectra in solvents of various polarity of BP-OC_{10} TP2 (A), BP-OC_{10} TP4 (B), BP-OC_{16} TP2 (C), and BP-OC_{16} TP4 (D). From polar to non-polar: methanol (purple), dimethyl sulfoxide (blue), tetrahydrofuran (green), chloroform (yellow), toluene (orange), cyclohexane (red).

Absorbance spectra in Figure S1 show a negligible shift for all derivatives when solvent polarity is changed. Probe concentrations were: 3 µM for TP2 dyes; 4 µM for TP4 dyes.

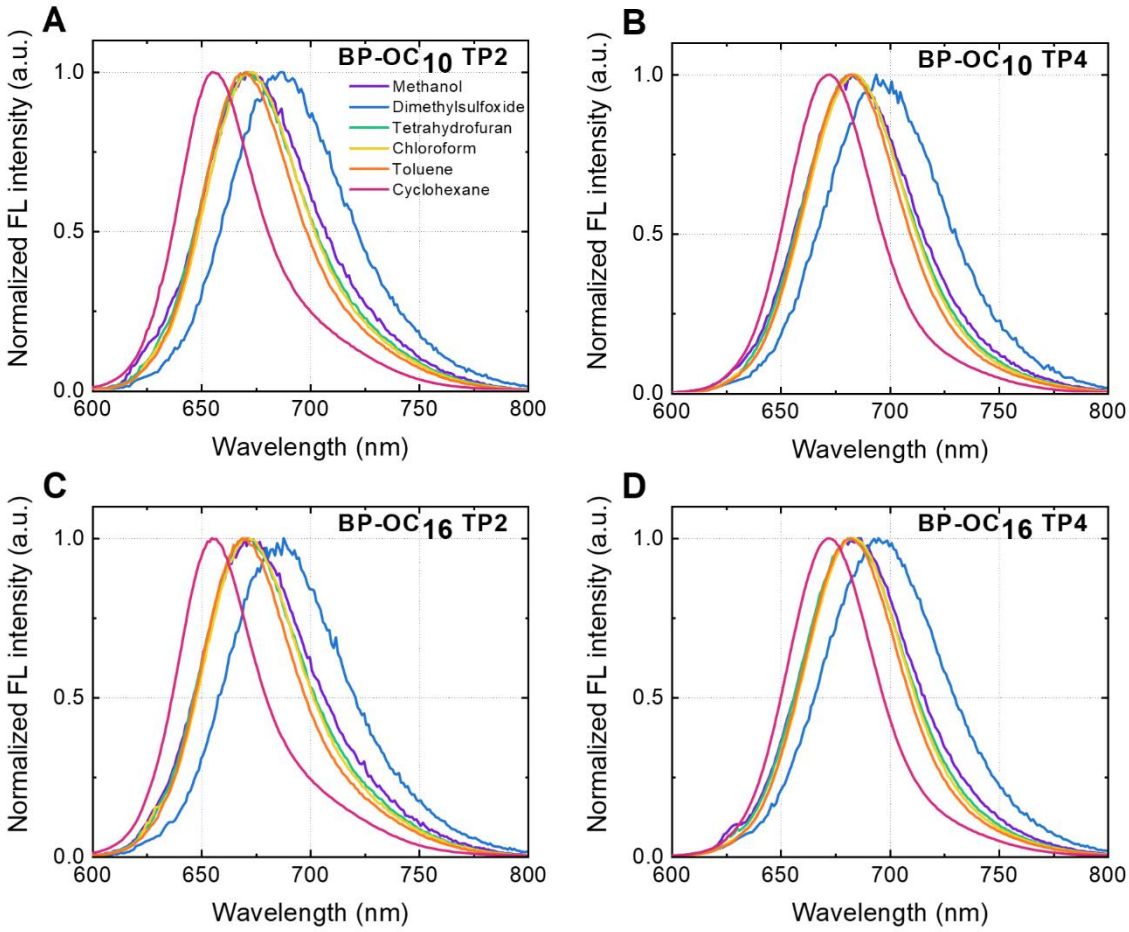

Figure S2. Normalised fluorescence spectra in solvents of various polarity of BP-OC_{10} TP2 (A), BP-OC_{10} TP4 (B), BP-OC_{16} TP2 (C), and BP-OC_{16} TP4 (D). From polar to non-polar: methanol (purple), dimethyl sulfoxide (blue), tetrahydrofuran (green), chloroform (yellow), toluene (orange), cyclohexane (red). Fluorescence spectra dependence on polarity.

Fluorescence spectra in Figure S2 show a weak solvatochromic shift when solvent polarity increased. The red-shift for disubstituted and tetrasubstituted dyes was 32 and 22 nm, respectively. Probe concentrations were: 3 µM for TP2 dyes; 4 µM for TP4 dyes.

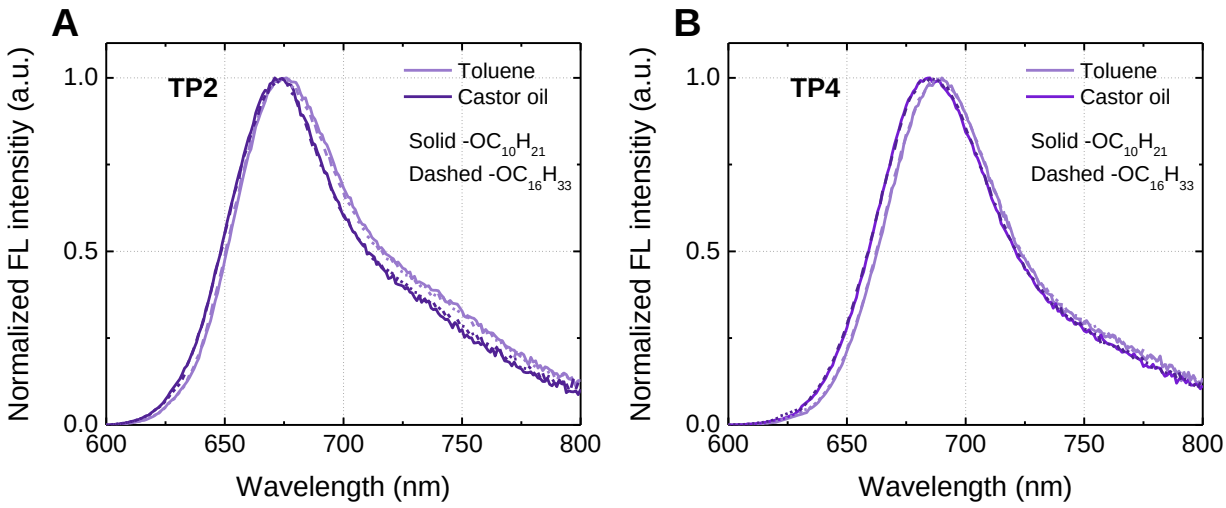

Figure S3. Fluorescence spectra dependence on viscosity for disubstituted (TP2) (A) and tetrasubstituted (TP4) probes (B) in non-polar toluene (light purple) and castor oil (dark purple) solvents. Solid lines correspond to -OC_{10} substituted, while dashed lines to -OC_{16} substituted derivatives.

Normalised fluorescence spectra of new derivatives depicted in Figure S3 shows that TP2- and TP4-substituted probes are viscosity insensitive. Probe concentrations were: 3 µM for TP2 dyes; 4 µM for TP4 dyes.

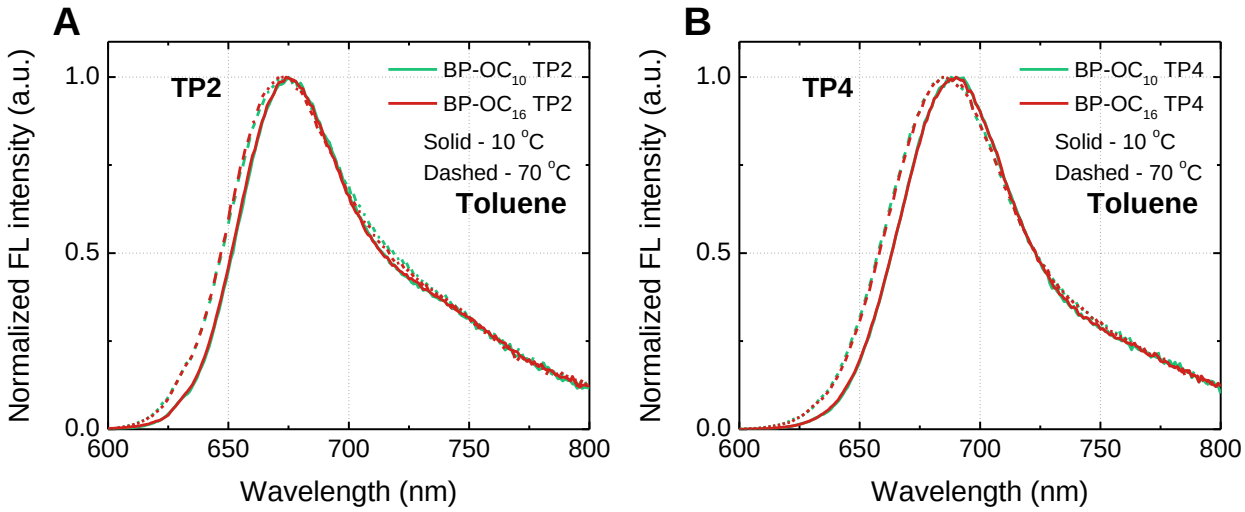

Figure S4. Fluorescence spectra dependence on temperature for disubstituted (TP2) (A) and tetrasubstituted (TP4) probes (B) in non-polar toluene solvent. Green lines correspond to -OC_{10} substituted, while red lines to -OC_{16} substituted derivatives. Solid lines correspond to 10 °C, while dashed lines to 70 °C temperature.

Figure S4 shows that the peak position of fluorescence spectrum shifts slightly to blue as temperature is increased. Probe concentrations were: 3 µM for TP2 dyes; 4 µM for TP4 dyes.

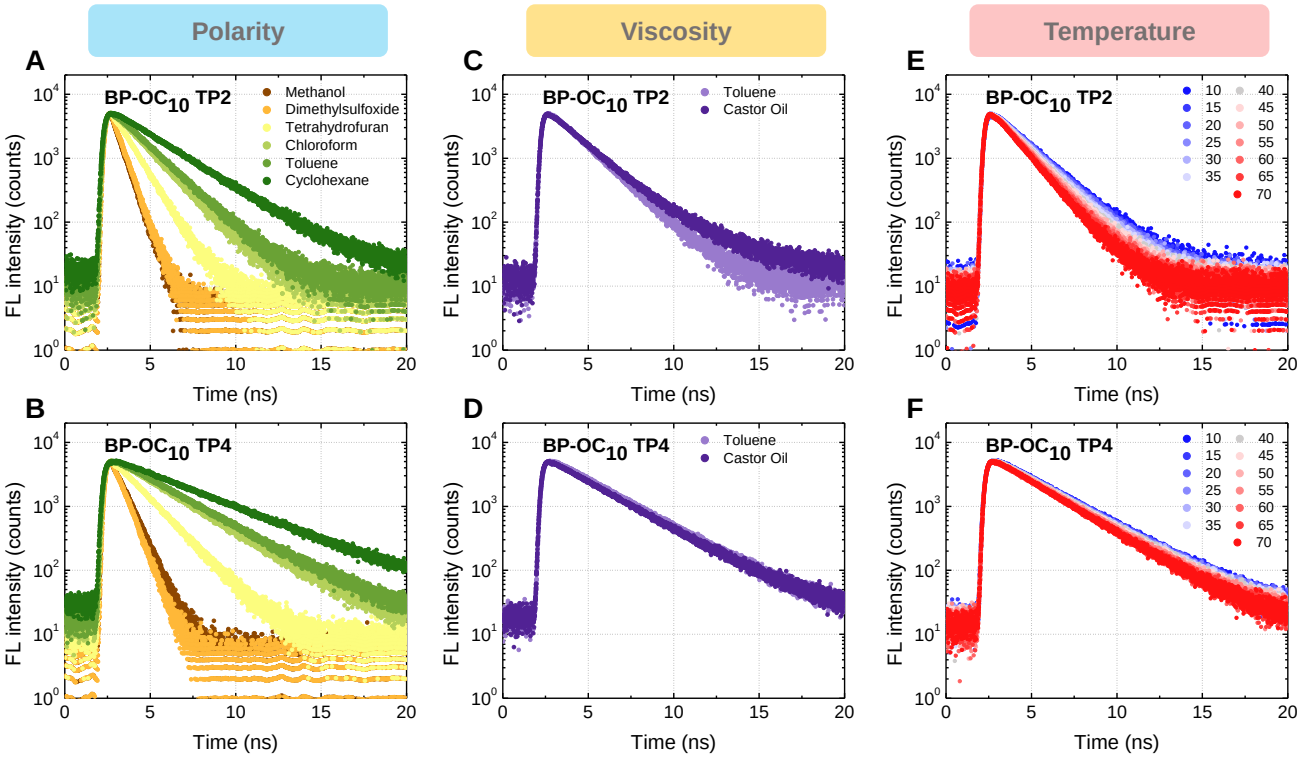

Figure S5. Time-resolved fluorescence measurements of BP-OC_{10} TP2 (A, C, E) and BP-OC_{10} TP4 (B, D, F), and their sensitivity to polarity (A-B), viscosity (C-D), and temperature (E-F). Abbreviations for the probes are given in the graphs.

Polarity dependence in solvents of differing polarity (A-B). Solvent polarity is quantified using their orientational polarizability (Equation (2), main text). Viscosity dependence in toluene and castor oil (C-D). Temperature dependence measured in toluene, range 10-70 °C (E-F).

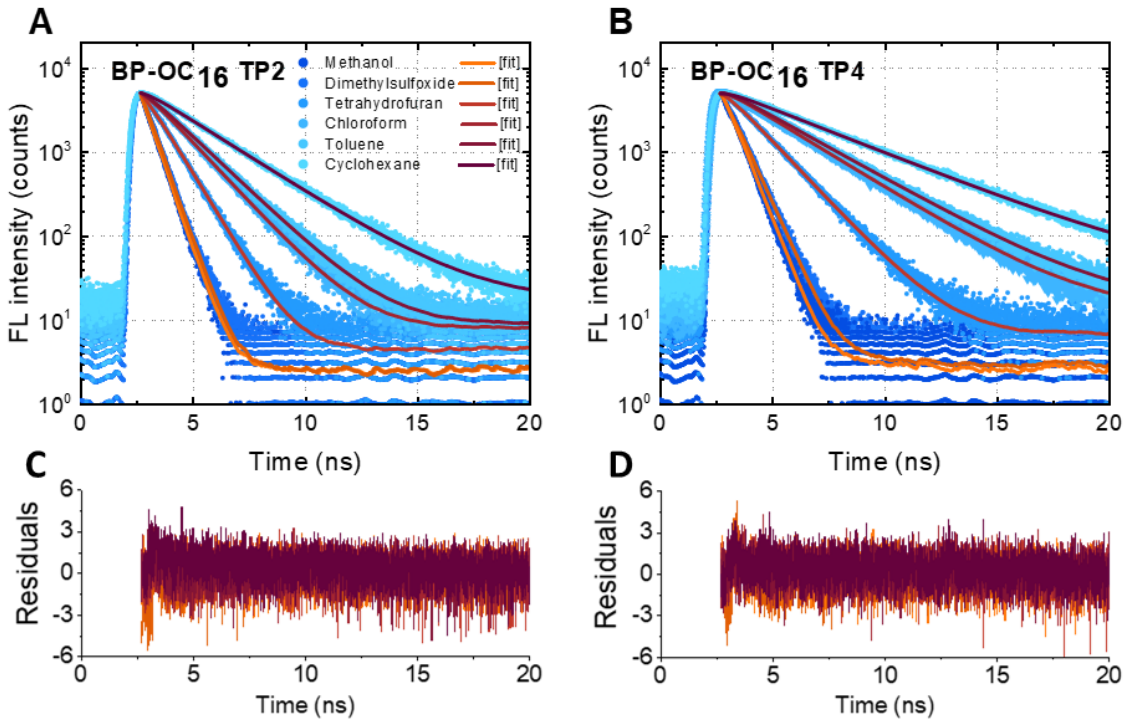

Figure S6. Fluorescence decays, fits and residuals of BP-OC_{16} TP2 *(A, C)* and BP-OC_{16} TP4 *(B, D)* in various solvents from very polar to apolar (methanol, dimethyl sulfoxide, tetrahydrofuran, chloroform, castor oil, toluene, cyclohexane). All decays were registered at 4096 channels. The fits of the decays are given at the interval from 550 to 4096 channels. The goodness-of-fit parameter (χ^2) was 1.5 or less. Decays are shown in blue, their fits and residuals in orange-purple colours.

Table S1. Fluorescence lifetime dependence on solvents polarity (Δf), fluorescence lifetime (τ) and goodness-of-fit parameter (χ^2) values of BP-OC_{10} TP2, BP-OC_{16} TP2, BP-OC_{10} TP4 and BP-OC_{16} TP4.

		SOLVENT						
		Methanol	**Dimethyl sulfoxide**	**Tetrahy-drofuran**	**Chloroform**	**Castor oil**	**Toluene**	**Cyclohexane**
Derivative	**Δf** / **Parameter**	0.3091	0.2833	0.2095	0.1479	0.1296	0.0136	0.0018
BP-OC_{10} TP2	τ, ns	0.45	0.48	0.96	1.51	2.04	1.70	2.55
	χ2	1.23	1.18	1.27	1.21	1.09	1.15	1.20
BP-OC_{10} TP4	τ, ns	0.68	0.56	1.53	2.63	2.84	2.89	4.07
	χ2	1.37	1.21	1.13	1.12	1.03	1.11	1.24
BP-OC_{16} TP2	τ, ns	0.46	0.49	0.95	1.48	2.07	1.66	2.55
	χ2	1.17	1.40	1.17	1.05	1.05	1.09	1.23
BP-OC_{16} TP4	τ, ns	0.67	0.56	1.52	2.64	2.85	2.90	4.09
	χ2	1.41	1.37	1.15	1.08	1.09	1.09	1.27

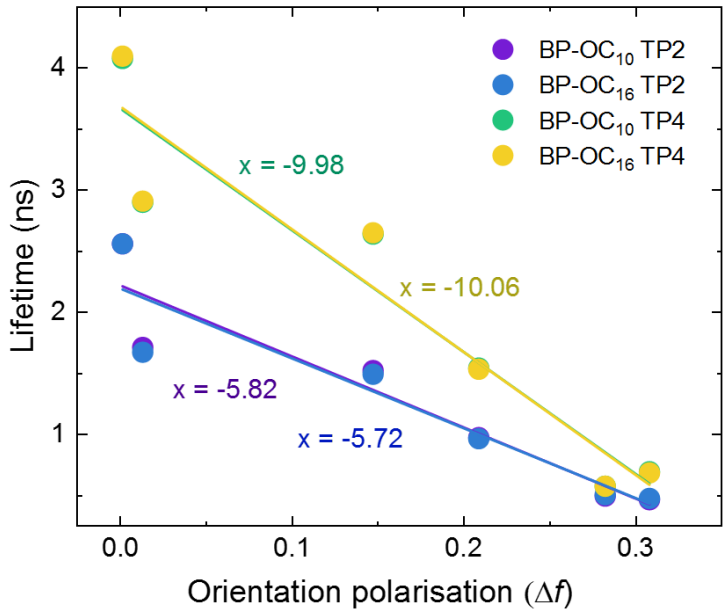

Figure S7. Fluorescence lifetimes of BP-OC_{10} TP2 (purple), BP-OC_{16} TP2 (blue), BP-OC_{10} TP4 (green) and BP-OC_{16} TP4 (yellow) obtained in the solvents of varying polarity. Slopes of the linear fits are displayed together. These experiments were performed in cyclohexane, toluene, chloroform, tetrahydrofuran, dimethyl sulfoxide and methanol (listed from non-polar to very polar).

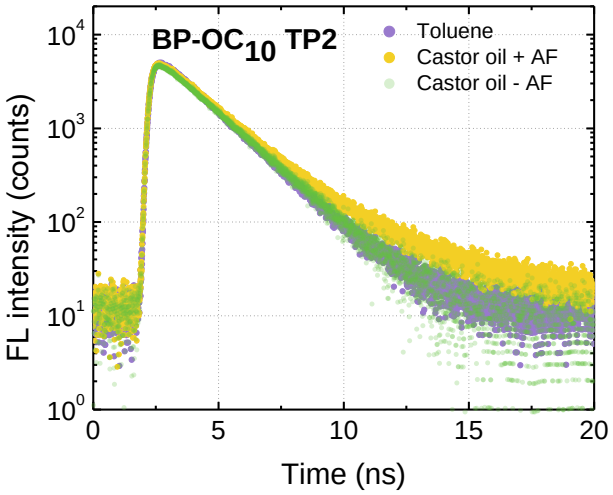

Figure S8. Fluorescence decays of BP-OC_{10} TP2 in toluene (light purple) and castor oil (yellow). Fluorescence decays are longer in castor oil because it shows some autofluorescence. To evaluate the fluorescence decay and lifetime of the dye in castor oil without its autofluorescence, the fluorescence decay of plain castor oil dye was subtracted from the fluorescence decay of the dye in castor oil (light green). The decays in toluene (light purple) and castor oil with autofluorescence subtracted (light green) overlaps, meaning that the probe is not affected by viscosity of the surrounding environment. The fluorescence decay of the pure castor oil was measured separately under identical experimental conditions, maintaining the same laser excitation intensity and acquisition time as for the sample with the fluorophore.

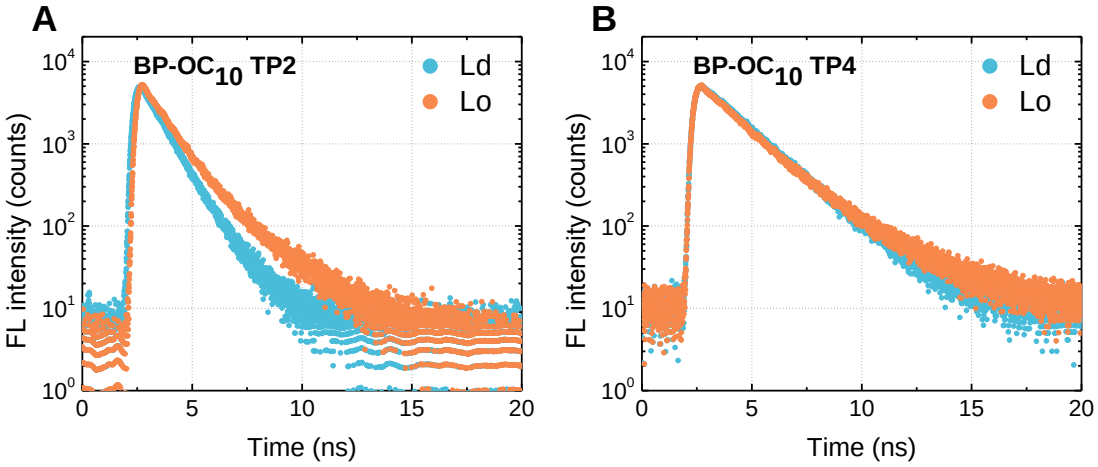

Figure S9. Fluorescence decays of BP-OC_{10} TP2 (A) and TP4 (B), measured in LUVs composed of DOPC (L_d phase; blue), DPPC : cholesterol : DOPC (5:5:1; L_o phase; orange).

Compared to -OC_{16} substituted probes that are discussed in the main text (Figure 4), -OC_{10} substituted probes show very similar properties. Fluorescence kinetics of the disubstituted dye also show ability to distinguish L_d and L_o lipid phases, while the tetrasubstituted dye has a negligible lifetime difference between the lipid phases.

2. Cellular imaging

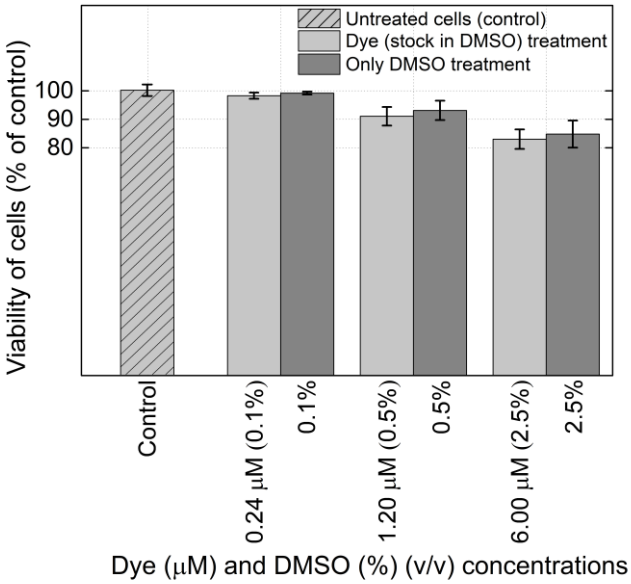

Figure S10. Viability of MCF-7 breast cancer cells after treatment with different concentrations of BP-OC_{16} TP2 (stock solution prepared in DMSO and then diluted in DPBS) or only DMSO diluted in DPBS for 30 min. The cells incubated in DPBS without BP-OC_{16} TP2 and DMSO served as a control group. Viability values were calculated from percentage values of cytotoxicity (N = 3, n = 3) determined by utilizing LDH assay. Results indicate that the observed cytotoxicity of BP-OC_{16} TP2 is mainly caused by the DMSO.

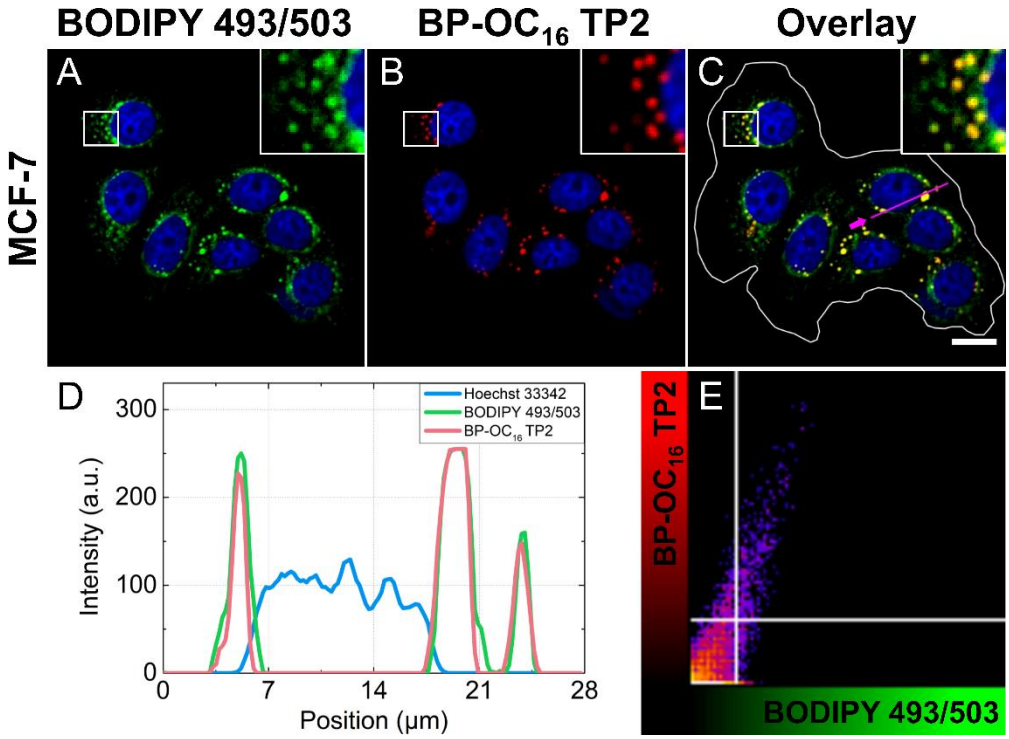

Figure S11. Colocalisation between a commercial LD stain – BODIPY 493/503 (λ_{ex} = 480±5 nm; detection range: 546±45 nm) (A) and BP-OC_{16} TP2 (λ_{ex} = 600±5 nm; detection range: 688±67 nm) (B), in live MCF-7 human breast cancer cells. The cells were also stained with Hoechst 33342 nuclei stain (λ_{ex} = 400±5 nm; detection range: 450±17 nm). C – overlay of green and red channels, scale bar – 15 µm. D – intensity profiles (blue – Hoechst 33342, green – BODIPY 493/503, red – BP-OC_{16} TP2) plotted along the drawn magenta line indicated by an arrow (C). E – fluorogram obtained from colocalisation analysis of MCF-7 cell colony selected as ROI (contours of the manually drawn ROI are shown as a white line in panel C). Pearson's correlation coefficient = 0.79, Manders' colocalisation coefficients: tM_1 = 0.79 (estimates the fraction of BODIPY 493/503 that colocalises with BP-OC_{16} TP2), tM_2 = 0.75 (estimates the fraction of BP-OC_{16} TP2 that colocalises with BODIPY 493/503).

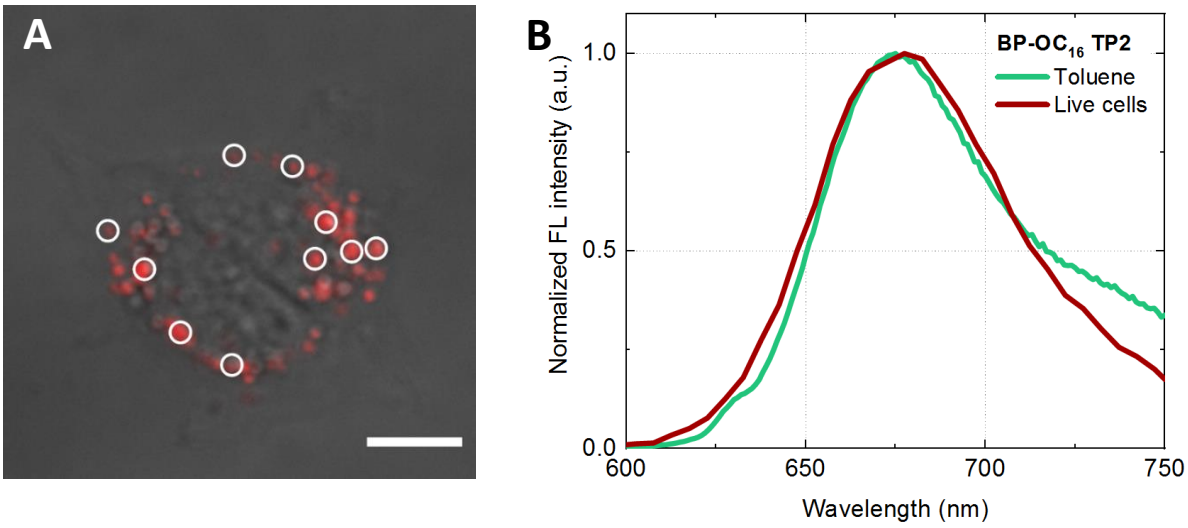

Figure S12. Comparison of BP-OC_{16} TP2 fluorescence spectrum from live MCF-7 breast cancer cells with a spectrum in toluene. A – brightfield image merged with a fluorescence image of a pair of MCF-7 cells stained with BP-OC_{16} TP2 (λ_{ex} = 410±5 nm). Scale bar – 10 µm. Fluorescence spectrum from the cells (B) was obtained by averaging fluorescence spectra measured with a 32-channel spectral detector from 10 different spots within cells (white circles in A), and subtracting the background fluorescence spectra, averaged from 3 different points.

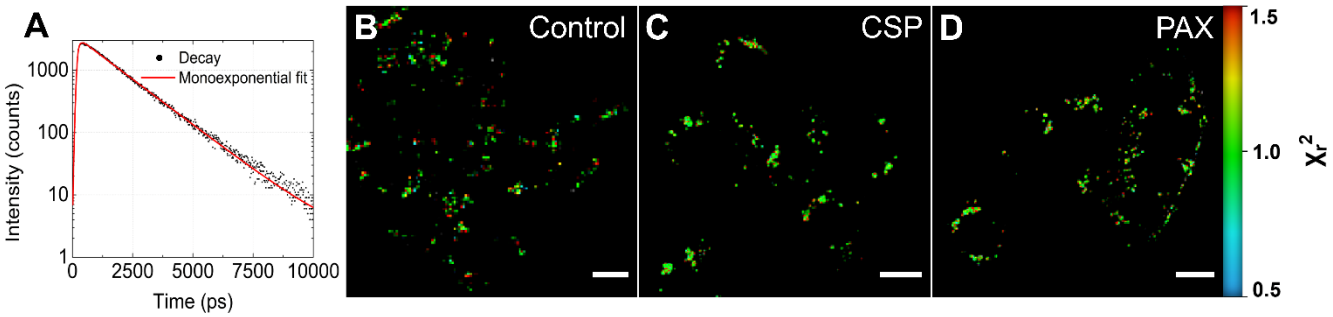

Figure S13. An example of a fluorescence decay (black) with a monoexponential fit (red line) (A) obtained from the FLIM image of live MCF-7 cells stained with BP-OC_{16} TP2 (Figure 5B, main text). χ_r^2 images (B-D) were obtained from the analysis of the FLIM images shown in Figure 5, main text. Scale bars – 15 µm. The average χ_r^2 values were 1.12, 1.26 and 1.25 for untreated, treated with 93 µM cisplatin (CSP) and treated with 7.2 nM paclitaxel (PAX) MCF-7 cells, respectively.

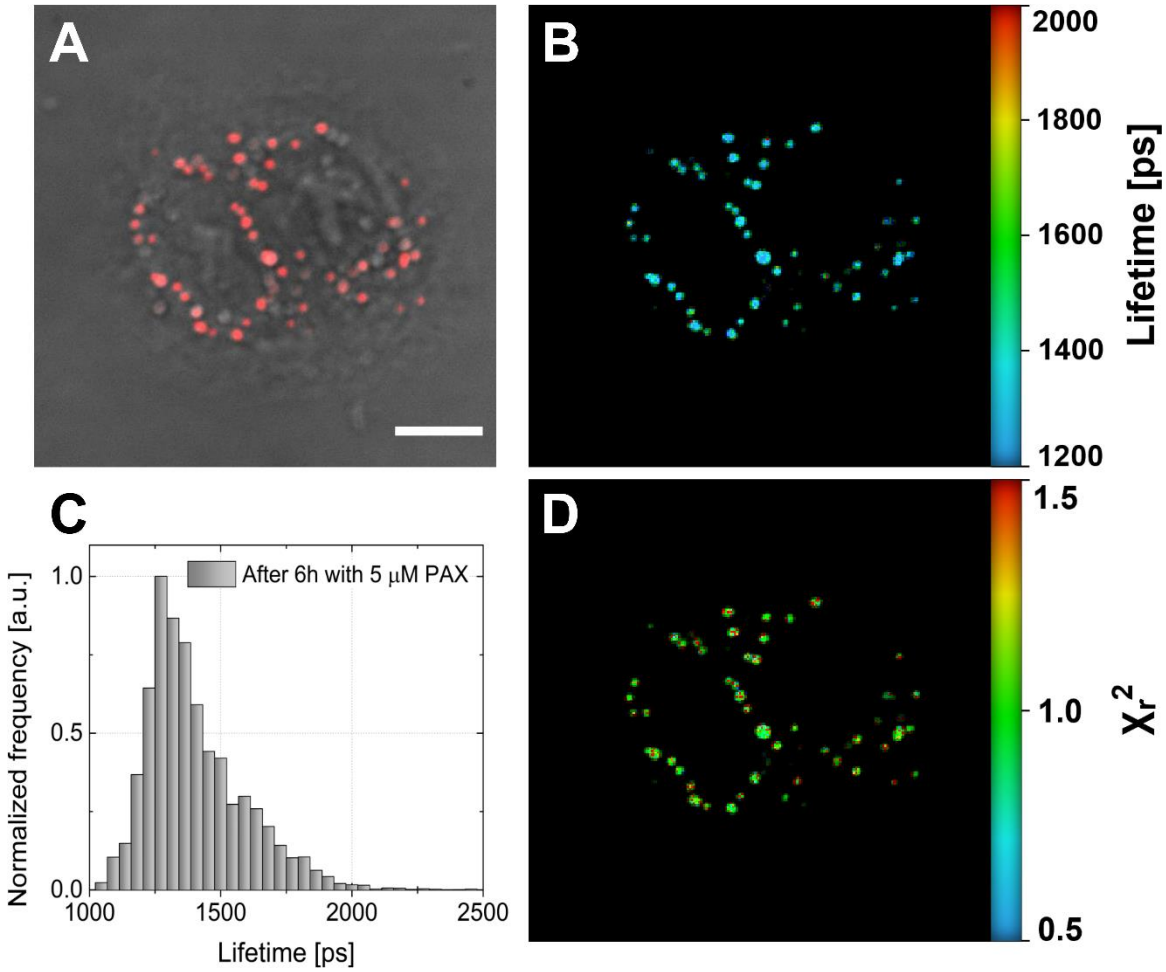

Figure S14. Application of BP-OC_{16} TP2 in live MCF-7 cells to monitor LD polarity after 6 h treatment with 5 μM PAX. A – confocal fluorescence image merged with brightfield image. Scale bar – 10 μm. B – FLIM image with LDs selected as ROI. C – lifetime histogram of the FLIM image. The mean lifetime is 1310 ps. D – χ_r^2 image obtained from the analysis of the aforementioned FLIM image. The average χ_r^2 value was 1.293. The fluorescence was excited at 410±5 nm and detected over the range of 621-755 nm.

3. Synthesis, compound characterisation, NMR and MS (MALDI-TOF) spectra

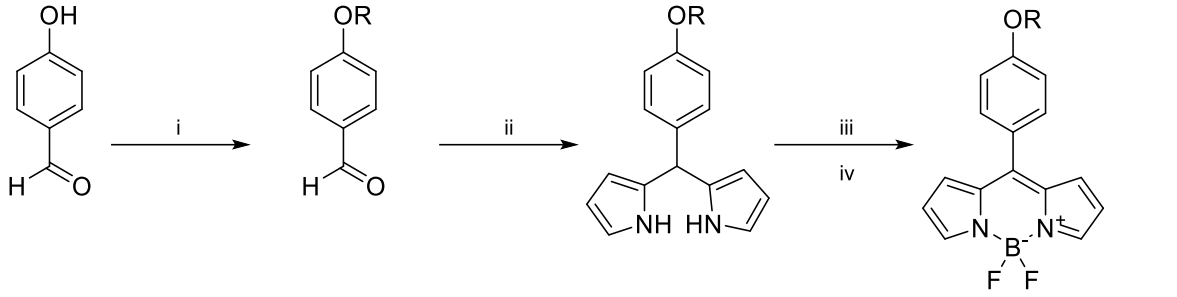

A R = $C_{10}H_{21}$ **C** R = $C_{10}H_{21}$ **BP-OC$_{10}$** R = $C_{10}H_{21}$
B R = $C_{16}H_{33}$ **D** R = $C_{16}H_{33}$ **BP-OC$_{16}$** R = $C_{16}H_{33}$

Scheme S1. ***Reagents and conditions****:* (i) 1 eq. 1-bromodecane or 1-bromohexadecane, 5 eq. K_2CO_3, DMF, argon, 80 °C, 2 h; (ii) neat pyrrole, TFA; (iii) 2 eq. DDQ, CH_2Cl_2, and then (iv) 7 eq. $BF_3{\cdot}(OEt_2)_2$, 7 eq. Et_3N, CH_2Cl_2, r.t., 24 h.

Compounds **A** [1] and **B** [2], dipyrromethanes **C-D** [3] and fluorophores **BP-OC$_{10}$**, **BP-OC$_{16}$** [4] were prepared according to previously published procedures.

BP-OC$_{16}$. Green-brown crystals, yield: 1.44 g (37%), mp 77-78 °C. ^{1}H NMR (400 MHz, $CDCl_3$): δ (ppm) = 7.94 (s, 2H), 7.55 (d, J = 8 Hz, 2H), 7.05 (d, J = 8 Hz, 2H), 7.01 (d, J = 4Hz, 2H), 6.58-6.56 (m, 2H), 4.07 (t, J = 6 Hz, 2H), 1.90-1.83 (m, 2H), 1.54-1.48 (m, 2H), 1.29-1.18 (m, 24H), 0.91 (t, J = 6 Hz, 3H); ^{13}C NMR (100 MHz, $CDCl_3$): δ (ppm) = 161.8; 143.3; 134.8; 132.5; 131.4; 129.0; 125.3; 118.2; 114.5; 68.4; 36.5; 31.9; 31.4; 29.7 (2); 29.68; 29.6; 29.59; 29.39; 29.38; 29.2; 26.1; 22.7; 21.5; 14.1; ^{19}F NMR (376.5 MHz, $CDCl_3$): δ (ppm) = -145.1 (q, J = 30.0 Hz); ^{11}B NMR (128.4 MHz, $CDCl_3$): δ = -0.30 (t, J = 28.2 Hz); **MS** (MALDI-TOF) m/z 509.32 ($C_{31}H_{43}BF_2N_2O$ $[M+H]^+$, requires 509.35).

Reaction scheme for disubstituted (TP2) dyes

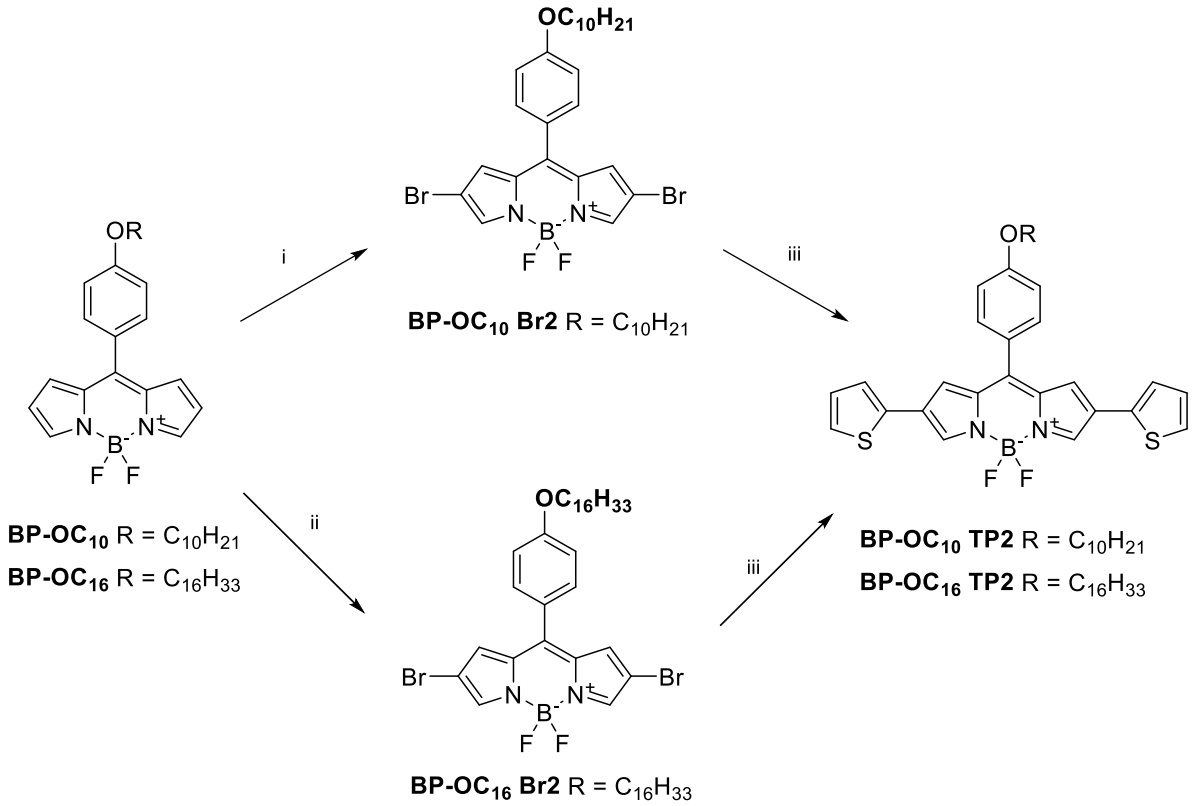

Scheme S2. ***Reagents and conditions****:* (i) 2.4 eq. NBS, CH_2Cl_2/DMF (1:1 vol%), r.t., 5 h; (ii) 3 eq. Br_2, CH_2Cl_2, r.t., 2 h; (iii) 3 eq. 2-(tributylstannyl)thiophene, 20 mol% $Pd(PPh_3)_4$, toluene, argon, 130 °C, 24 h.

Fluorophore **BP-OC$_{10}$ Br2** was synthesized according to previously published procedures [5].

BP-OC$_{16}$ Br2. To a solution of **BP-OC$_{16}$** (101 mg, 0.20 mmol) in CH_2Cl_2 (15 mL) 3 eq. of Br_2 (30.5 µL, 0.60 mmol) dissolved in CH_2Cl_2 (5 mL) were added dropwise. The mixture was stirred at room temperature for 2 h until the total consumption of the reagents. The reaction progress was controlled using thin-layer chromatography. After the reaction was complete, the solvent was removed under reduced pressure and the crude product was purified by column chromatography on silica gel (eluent - petroleum ether:chloroform, 3:2) to give **BP-OC$_{16}$ Br2** as a red solid.

BP-OC$_{16}$ Br2. Red crystals, yield: 121 mg (91%), mp 107-108 °C. ^{1}H NMR (400 MHz, $CDCl_3$): δ (ppm) = 7.84 (s, 2H), 7.54 (d, J = 8 Hz, 2H), 7.07 (d, J = 8 Hz, 2H), 7.02 (s, 2H), 4.08 (t, J = 8 Hz, 2H), 1.90-1.83 (m, 2H), 1.53-1.48 (m, 2H), 1.32-1.28 (m, 24H), 0.90 (t, J = 6 Hz, 3H); ^{13}C NMR (100 MHz, $CDCl_3$): δ (ppm) = 162.6, 143.2, 134.5, 132.6, 132.5, 131.5, 125.2, 114.97, 106.8, 68.5, 31.9, 29.7 (4), 29.67 (2), 29.6, 29.58, 29.4 (2), 29.1, 26.0, 22.7, 14.1; ^{19}F NMR (376.5 MHz, $CDCl_3$): δ (ppm) = -145.0 (q, J = 30.1 Hz); ^{11}B NMR (128.4 MHz, $CDCl_3$): δ = -0.26 (t, J = 28.9 Hz); **MS** (MALDI-TOF) m/z 667.23 ($C_{31}H_{41}BBr_2F_2N_2O$ $[M+H]^+$, requires 667.17).

BP-OC$_{10}$ (C$_{16}$) TP2. To a solution of **BP-OC$_{10}$ Br2** (101 mg, 0.17 mmol) or **BP-OC$_{16}$ Br2** (100 mg, 0.15 mmol) in toluene (2 mL) catalyst $Pd(PPh_3)_4$ (20 mol%) was added under argon atmosphere. Afterwards, 3 eq. of 2-(tributylstannyl)thiophene were added through a syringe

and the mixture was heated at 130 °C for 24 h. The reaction progress was controlled using thin-layer chromatography. After it was complete, the mixture was cooled down to room temperature and toluene was removed under reduced pressure. The residue was taken up in CH_2Cl_2, washed with water and brine, and then dried over anhydrous Na_2SO_4. Finally, the crude product was purified by column chromatography on silica gel (eluent - petroleum ether:chloroform, 1:2) to give **BP-OC$_{10}$ TP2** and **BP-OC$_{16}$ TP2** as green solids.

BP-OC$_{10}$ TP2. Green crystals, yield: 95 mg (92%), mp 177-178 °C. ^{1}H NMR (400 MHz, $CDCl_3$): δ (ppm) = 8.19 (s, 2H), 7.63 (d, J = 8 Hz, 2H), 7.26-7.24 (m, 2H), 7.20-7.19 (m, 2H), 7.12 (d, J = 8 Hz, 2H), 7.07-7.05 (m, 2H), 7.03 (s, 2H), 4.11 (t, J = 6 Hz, 2H), 1.91-1.87 (m, 2H), 1.54-1.52 (m, 2H), 1.43-1.3 (m, 12H), 0.92 (t, J = 6 Hz, 3H); ^{13}C NMR (100 MHz, $CDCl_3$): δ (ppm) = 162.0, 141.1, 135.9, 135.4, 132.5, 128.1, 127.9, 124.7, 124.3, 123.3 (2), 114.8, 68.5, 31.9, 29.6, 29.58, 29.4, 29.3, 29.2, 26.1, 22.7, 14.1; ^{19}F NMR (376.5 MHz, $CDCl_3$): δ (ppm) = -145.2 (q, J = 26.4 Hz); ^{11}B NMR (128.4 MHz, $CDCl_3$): δ (ppm) = 0.14 (t, J = 30.5 Hz); **MS** (MALDI-TOF) m/z 589.22 ($C_{33}H_{35}BF_2N_2OS_2$ $[M+H]^+$, requires 589.23).

BP-OC$_{16}$ TP2. Green crystals, yield: 91 mg (91%), mp 162-163 °C. ^{1}H NMR (400 MHz, $CDCl_3$): δ (ppm) = 8.09 (s, 2H), 7.53 (d, J = 8 Hz, 2H), 7.16-7.14 (m, 2H), 7.11-7.09 (m, 2H), 7.02 (d, J = 8 Hz, 2H), 6.98-6.96 (m, 2H), 6.93 (s, 2H), 4.02 (t, J = 6 Hz, 2H), 1.81-1.77 (m, 2H), 1.46-1.42 (m, 2H), 1.25-1.19 (m, 24H), 0.81 (t, J = 6 Hz, 3H); ^{13}C NMR (100 MHz, $CDCl_3$): δ (ppm) = 162.0, 141.1, 135.9, 135.4, 132.5, 128.1, 127.9, 125.9, 124.7, 124.3, 123.3 (2), 114.8, 68.5, 31.9, 29.7 (4), 29.68 (2), 29.63, 29.61, 29.4, 29.38, 29.2, 26.1, 22.7, 14.1; ^{19}F NMR (376.5 MHz, $CDCl_3$): δ (ppm) = -145.2 (q, J = 26.4 Hz); ^{11}B NMR (128.4 MHz, $CDCl_3$): δ (ppm) = 0.14 (t, J = 30.5 Hz); **MS** (MALDI-TOF) m/z 673.17 ($C_{39}H_{47}BF_2N_2OS_2$ $[M+H]^+$, requires 673.33).

Reaction scheme for tetrasubstituted (TP4) dyes

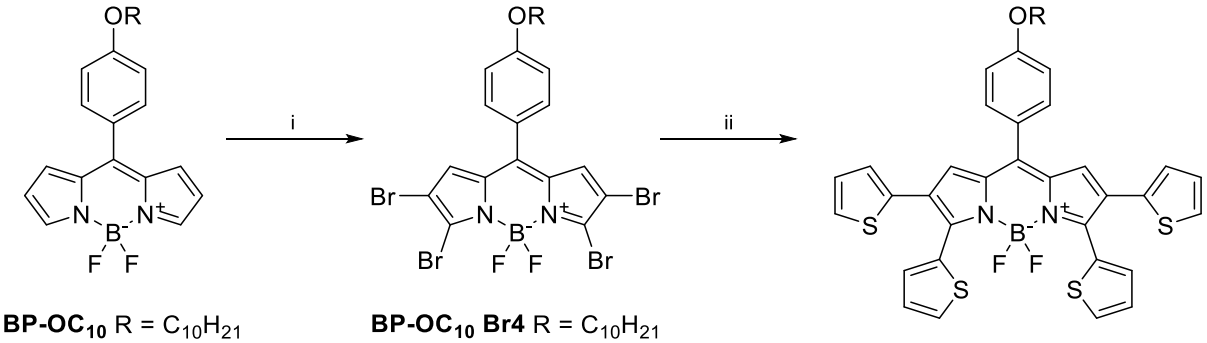

BP-OC$_{10}$ R = $C_{10}H_{21}$
BP-OC$_{16}$ R = $C_{16}H_{33}$

BP-OC$_{10}$ Br4 R = $C_{10}H_{21}$
BP-OC$_{16}$ Br4 R = $C_{16}H_{33}$

BP-OC$_{10}$ TP4 R = $C_{10}H_{21}$
BP-OC$_{16}$ TP4 R = $C_{16}H_{33}$

Scheme S3. ***Reagents and conditions:*** (i) 6 eq. Br_2, CH_2Cl_2, r.t., 3 h; (ii) 6 eq. 2-(tributylstannyl)thiophene, 20 mol% $Pd(PPh_3)_4$, toluene, argon, 130 °C, 24 h.

BP-OC$_{10}$ (C$_{16}$) Br4. To a solution of **BP-OC$_{10}$** (100 mg, 0.236 mmol) or **BP-OC$_{16}$** (100 mg, 0.197 mmol) in CH_2Cl_2 (15 mL) 6 eq. of Br_2 dissolved in CH_2Cl_2 (5 mL) were added dropwise. The mixture was stirred at room temperature for 3 h until the reagents were fully converted into the product. The reaction progress was controlled using thin-layer chromatography. After the reaction was complete, solvents were removed under reduced pressure and the crude product was purified by column chromatography on silica gel (eluent - petroleum ether:chloroform, 1:1) to give **BP-OC$_{10}$ Br4** and **BP-OC$_{16}$ Br4** as dark-red solids.

BP-OC$_{10}$ Br4. Dark-red crystals, yield: 161 mg (92%), mp 157-158 °C. ^{1}H NMR (400 MHz, $CDCl_3$): δ (ppm) = 7.24 (d, J = 8 Hz, 2H), 6.85 (d, J = 8 Hz, 2H), 6.76 (s, 2H), 3.86 (t, J = 8 Hz, 2H), 1.67-1.61 (m, 2H), 1.32-1.26 (m, 2H), 1.21-1.06 (m, 12H), 0.70 (t, J = 8 Hz, 3H); ^{13}C NMR (100 MHz, $CDCl_3$): δ (ppm) = 162.4, 143.2, 134.6, 133.9, 132.4, 131.4, 123.9, 115.0, 111.6, 68.5, 31.9, 29.6, 29.58, 29.36, 29.34, 29.1, 26.0, 22.7, 14.2; ^{19}F NMR (376.5 MHz, $CDCl_3$): δ (ppm) = -148.07 (q, J = 26.4 Hz); ^{11}B NMR (128.4 MHz, $CDCl_3$): δ (ppm) = 0.21 (t, J = 28.2 Hz); **MS** (MALDI-TOF) m/z 740.96 ($C_{25}H_{27}BBr_4F_2N_2O$ $[M+H]^+$, requires 740.90).

BP-OC$_{16}$ Br4. Dark-red crystals, yield: 148 mg (92%), mp 135-136 °C. ^{1}H NMR (400 MHz, $CDCl_3$): δ (ppm) = 7.46 (d, J = 8 Hz, 2H), 7.06 (d, J = 8 Hz, 2H), 6.98 (s, 2H), 4.07 (t, J = 6 Hz, 2H), 1.90-1.83 (m, 2H), 1.53-1.49 (m, 2H), 1.37-1.28 (m, 24H), 0.90 (t, J = 6 Hz, 3H); ^{13}C NMR (100 MHz, $CDCl_3$): δ (ppm) = 162.4, 143.2, 134.6, 133.9, 132.4, 131.4, 123.9, 115.0, 111.6, 68.5, 31.9, 29.7 (4), 29.68 (2), 29.6, 29.5 (2), 29.1, 26.0, 22.7, 14.1; ^{19}F NMR (376.5 MHz, CDCl3) δ (ppm) = -148.1 (q, J = 26.4 Hz); ^{11}B NMR (128.4 MHz, $CDCl_3$): δ (ppm) = 0.22 (t, J = 26.9 Hz); **MS** (MALDI-TOF) m/z 825.08 ($C_{31}H_{39}BBr_4F_2N_2O$ $[M+H]^+$, requires 824.99).

BP-OC$_{10}$ (C$_{16}$) TP4. To a solution of **BP-OC$_{10}$ Br4** (50 mg, 0.068 mmol) or **BP-OC$_{16}$ Br4** (50 mg, 0.061 mmol) in toluene (2 mL) catalyst $Pd(PPh_3)_4$ (20 mol%) was added under argon atmosphere. Afterwards 6 eq. of 2-(tributylstannyl)thiophene were added through a syringe and the mixture was heated at 130 °C for 24 h. The reaction progress was controlled using thin-layer chromatography. After it was complete, the mixture was cooled down to room temperature and toluene was removed under reduced pressure. The residue was taken up in CH_2Cl_2, washed with water and brine, and then dried over anhydrous Na_2SO_4. Finally, the

crude product was purified by column chromatography on silica gel (eluent - petroleum ether:chloroform, 1:1) to give **BP-OC$_{10}$ TP4** and **BP-OC$_{16}$ TP4** as green solids.

BP-OC$_{10}$ TP4. Green crystals, yield: 50 mg (99%), mp 84-85 ^{o}C. ^{1}H NMR (400 MHz, $CDCl_3$): δ (ppm) = 7.39 (d, *J* = 8 Hz, 2H), 7.34-7.32 (m, 2H), 7.30-7.29 (m, 2H), 7.01-6.99 (m, 2H), 6.91-6,87 (m, 4H), 6.82 (s, 2H), 6.73-6.71 (m, 2H), 6.57-6.55 (m, 2H), 3.88 (t, *J* = 6 Hz, 2H), 1.68-1.65 (m, 2H), 1.37-1.32 (m, 2H), 1.17-1.10 (m, 12H), 0.71 (t, *J* = 6 Hz, 3H); ^{13}C NMR (100 MHz, $CDCl_3$): δ (ppm) = 161.5, 148.4, 143.8, 135.4, 135.0, 132.4, 132.2, 131.1, 129.5, 128.8, 128.0, 127.3, 127.2, 126.2, 126.1, 125.5, 114.7, 68.4, 31.9, 29.62, 29.60, 29.4, 29.36, 29.2, 26.1, 22.7, 14.2; ^{19}F NMR (376.5 MHz, $CDCl_3$): δ (ppm) = -135.2 (q, *J* = 30.1 Hz); ^{11}B NMR (128.4 MHz, $CDCl_3$): δ (ppm) = 0.95 (t, *J* = 30.8 Hz); **MS** (MALDI-TOF) m/z 753.12 ($C_{41}H_{39}BF_2N_2OS_4$ $[M+H]^+$, requires 753.21).

BP-OC$_{16}$ TP4. Green crystals, yield: 46 mg (91%), mp 104-105 ^{o}C. ^{1}H NMR (400 MHz, $CDCl_3$): δ (ppm) = 7.84 (d, J = 8 Hz, 2H), 7.78-7.76 (m, 2H), 7.75-7.73 (m, 2H), 7.45-7.44 (m, 2H), 7.36-7.32 (m, 4H), 7.26 (s, 2H), 7.18-7.16 (m, 2H), 7.01 (d, J = 4 Hz, 2H), 4.32 (t, J = 6 Hz, 2H), 2.13-2.09 (m, 2H), 1.78-1.74 (m, 2H), 1.64-1.48 (m, 24H), 1.1 (t, J = 6 Hz, 3H); ^{13}C NMR (100 MHz, $CDCl_3$): δ (ppm) = 161.5, 148.4, 135.4, 135.0, 132.4, 132.2, 131.1, 129.5, 128.8; 127.99, 127.23, 127.21, 126.15, 126.11; 125.4, 114.6, 68.4, 31.9, 29.7 (4), 29.69 (2), 29.64, 29.62, 29.4, 29.38, 29.2, 26.1, 22.7, 14.1. ^{19}F NMR (376.5 MHz, $CDCl_3$): δ (ppm) = -135.2 (q, J = 30.1 Hz); ^{11}B NMR (128.4 MHz, $CDCl_3$): δ (ppm) = 0.94 (t, J = 29.5 Hz); **MS** (MALDI-TOF) m/z 837.30 ($C_{47}H_{51}BF_2N_2OS_4$ $[M+H]^+$, requires 837.30).

NMR and Mass Spectrometry (MALDI-TOF) spectra

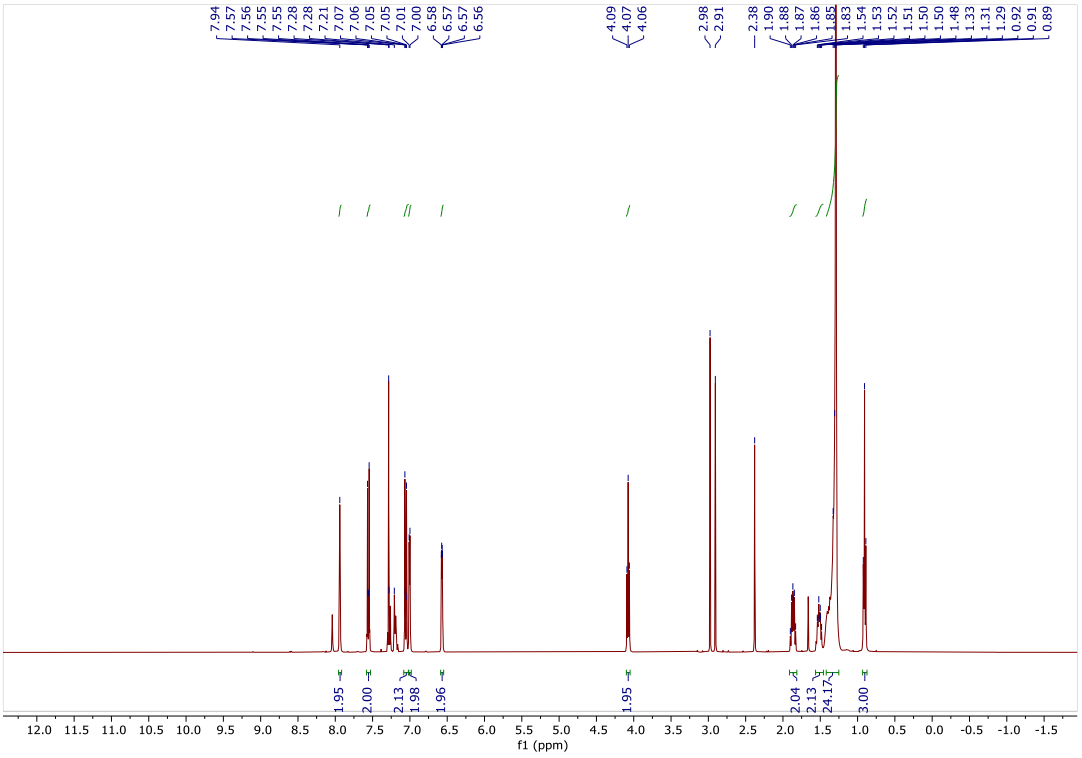

Figure S15. ^{1}H NMR spectrum of **BP-OC$_{16}$**.

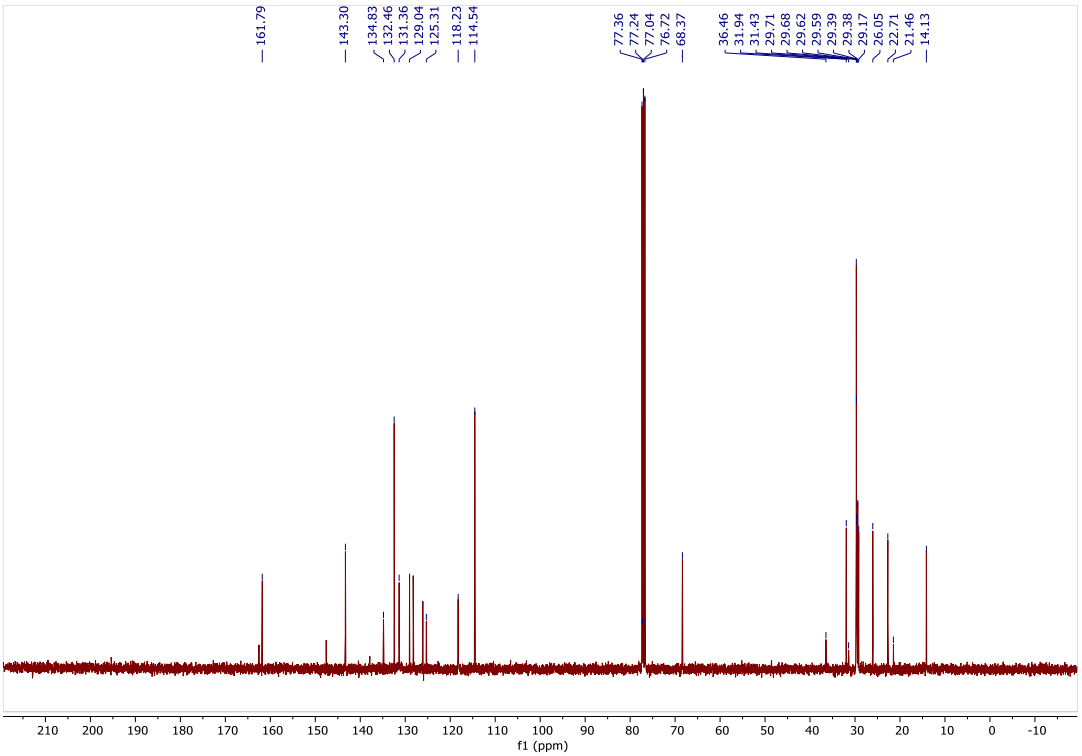

Figure S16. ^{13}C NMR spectrum of **BP-OC$_{16}$**.

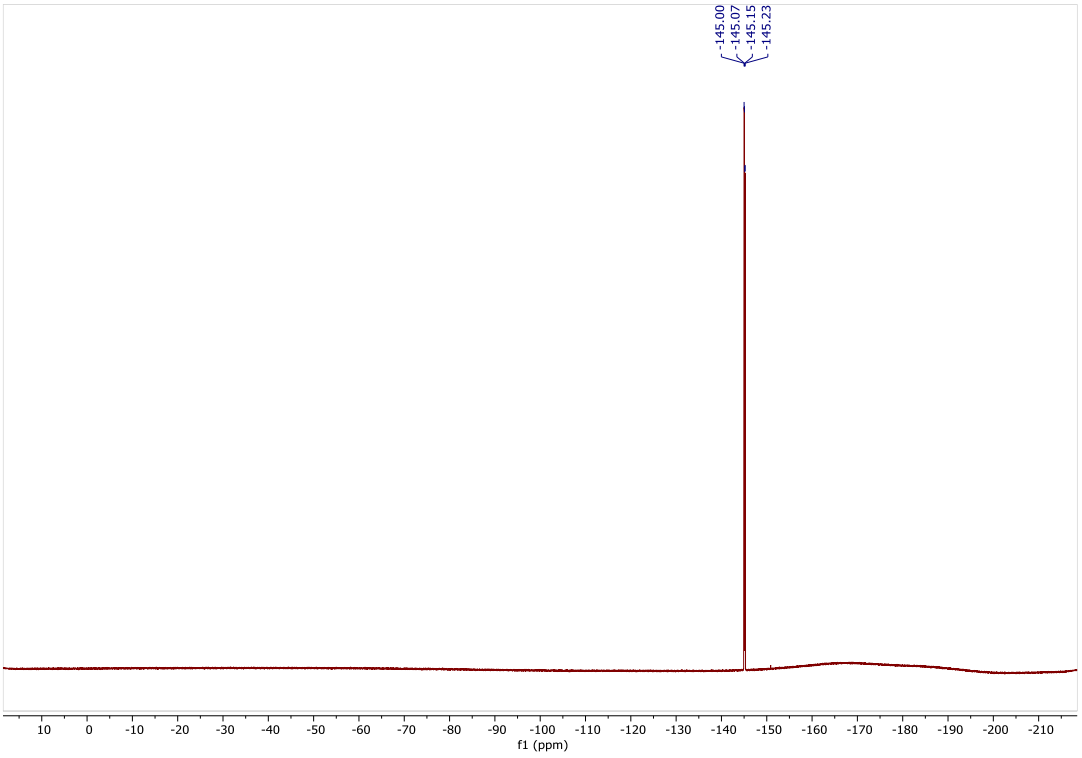

Figure S17. ^{19}F NMR spectrum of **BP-OC$_{16}$**.

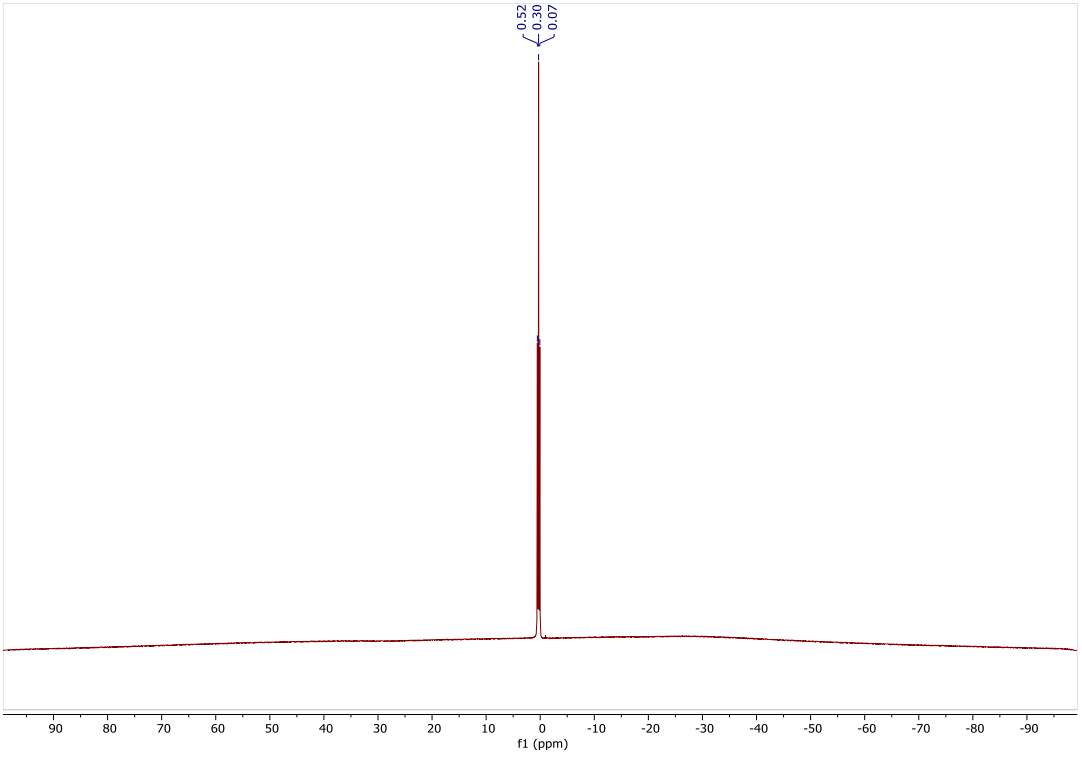

Figure S18. ^{11}B NMR spectrum of **BP-OC$_{16}$**.

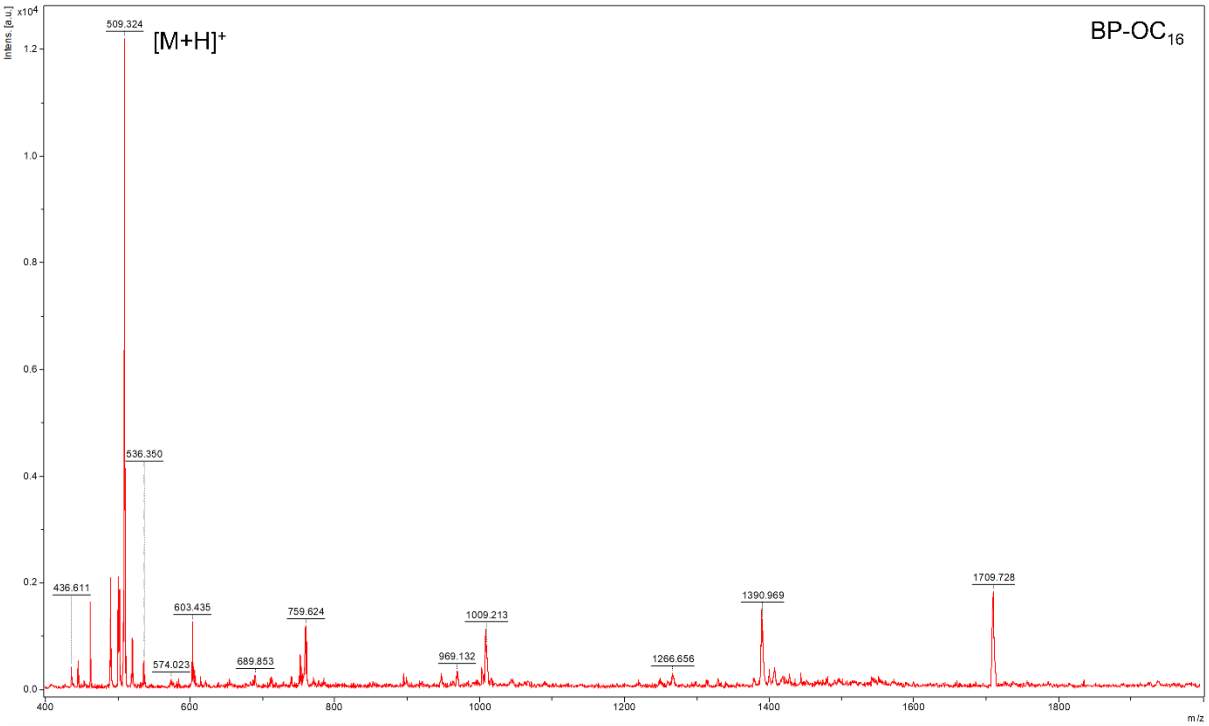

Figure S19. MS spectrum of **BP-OC$_{16}$.**

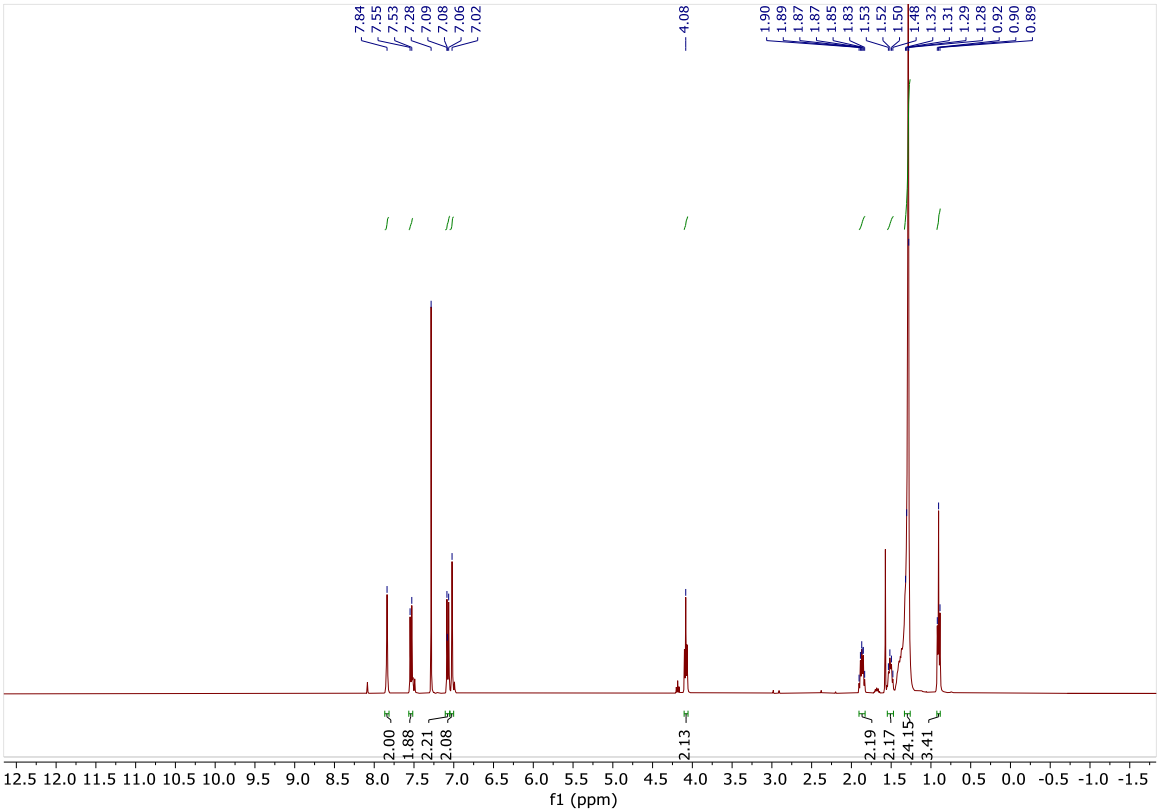

Figure S20. ^{1}H NMR spectrum of **BP-OC$_{16}$ Br2**.

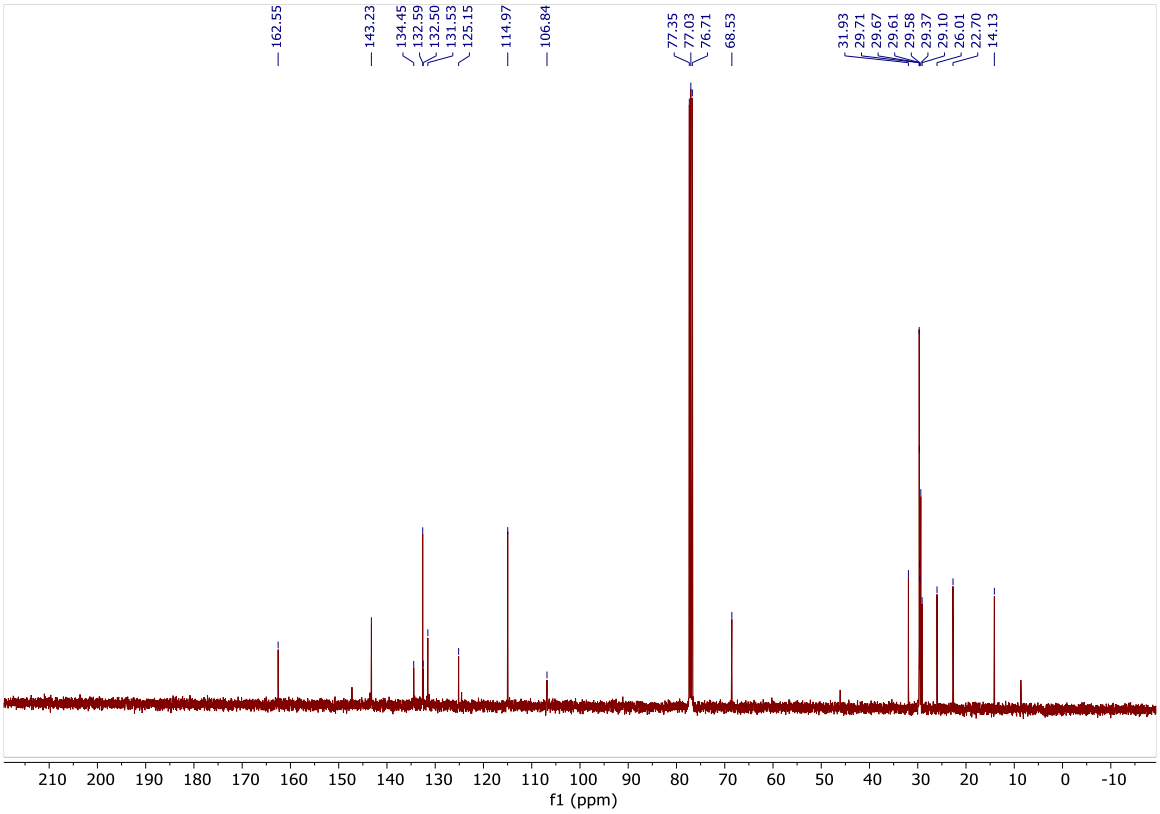

Figure S21. ^{13}C NMR spectrum of **BP-OC$_{16}$ Br2**.

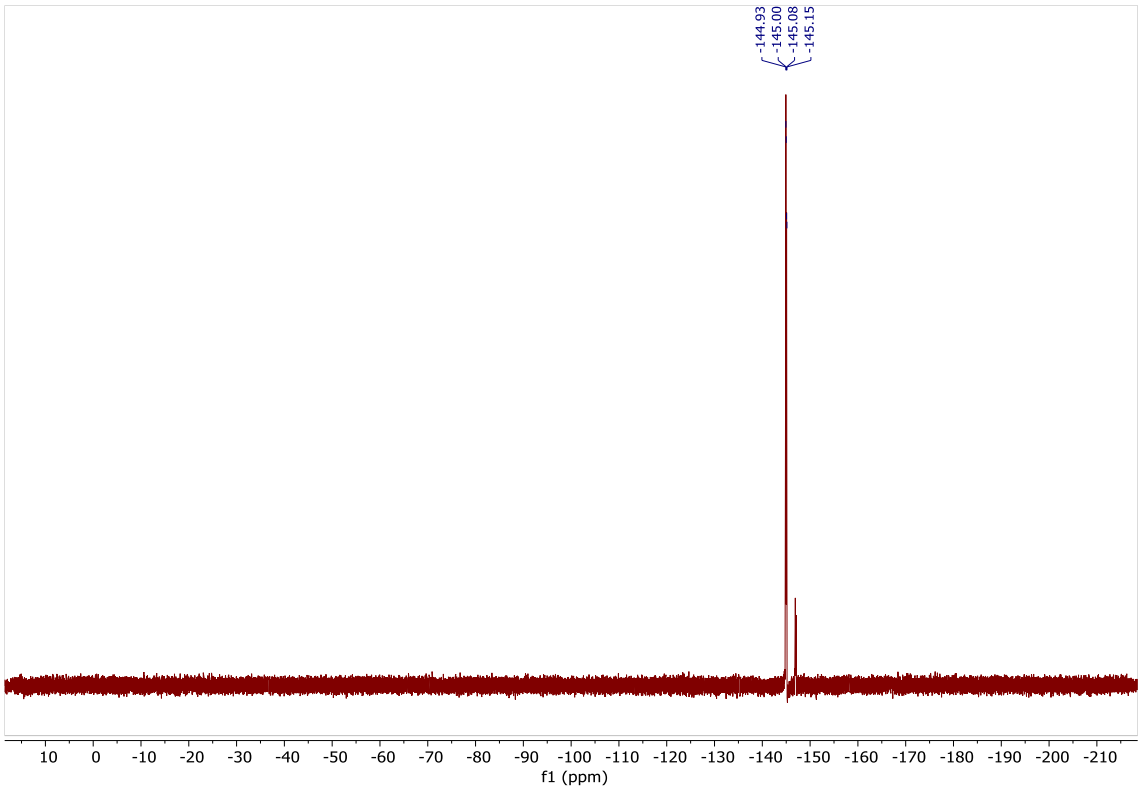

Figure S22. ^{19}F NMR spectrum of **BP-OC$_{16}$ Br2**.

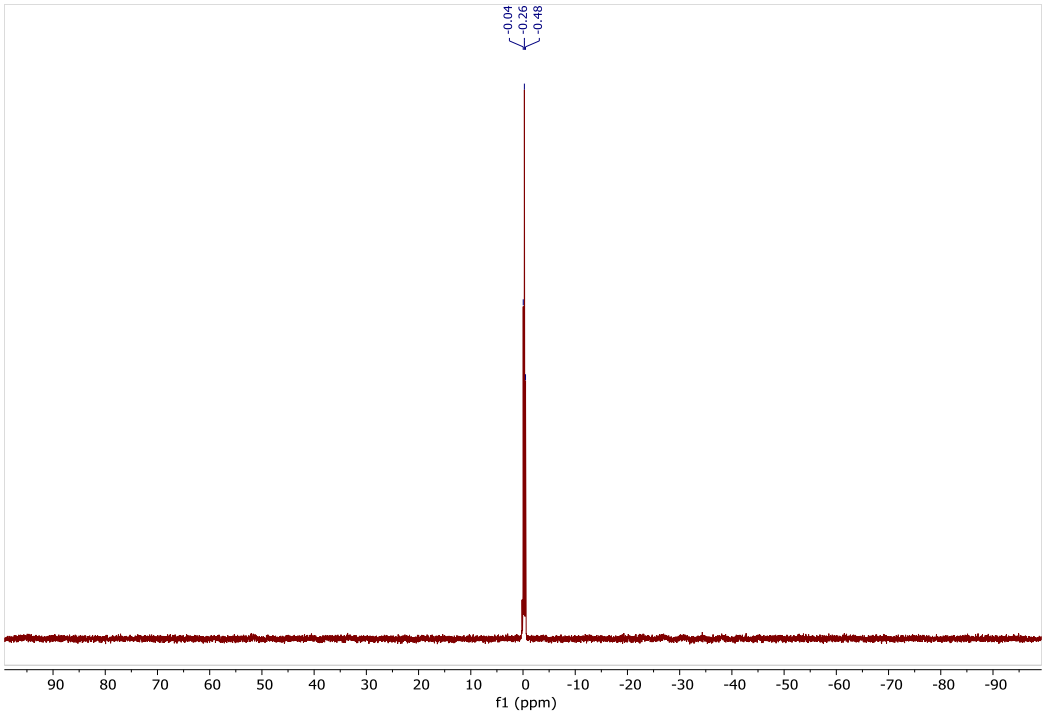

Figure S23. ^{11}B NMR spectrum of **BP-OC$_{16}$ Br2**.

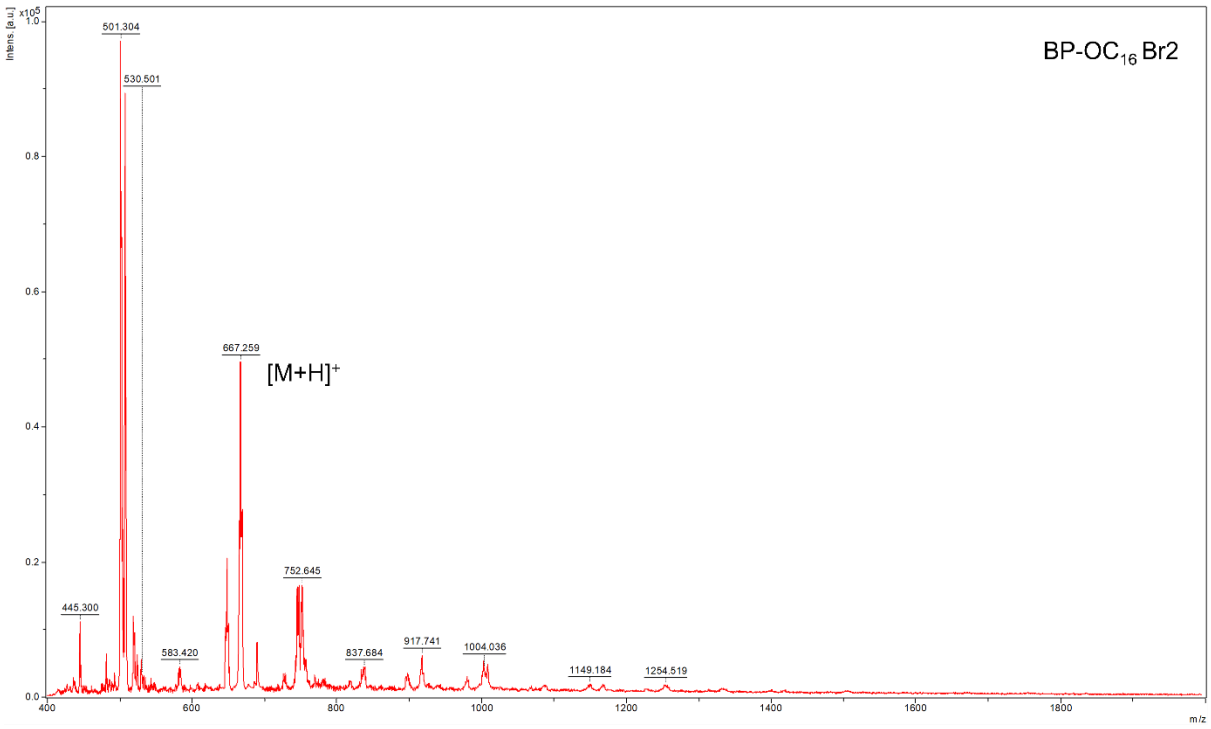

Figure S24. MS spectrum of **BP-OC$_{16}$ Br2.**

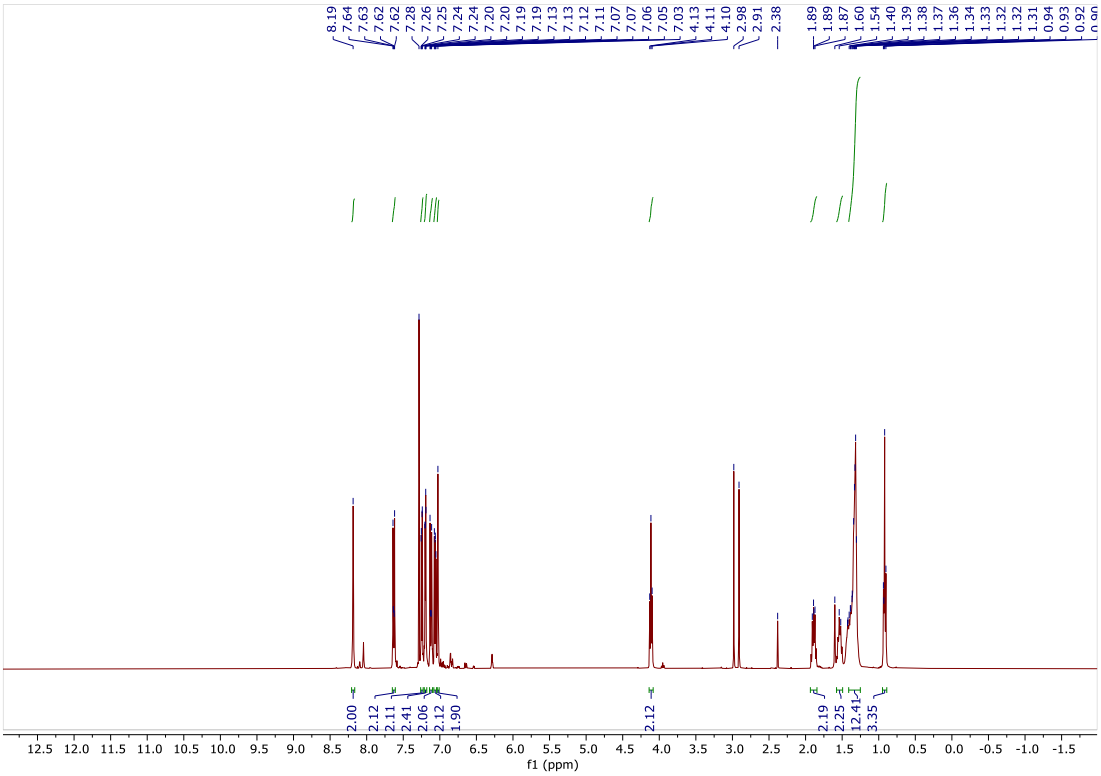

Figure S25. ^{1}H NMR spectrum of **BP-OC$_{10}$ TP2**.

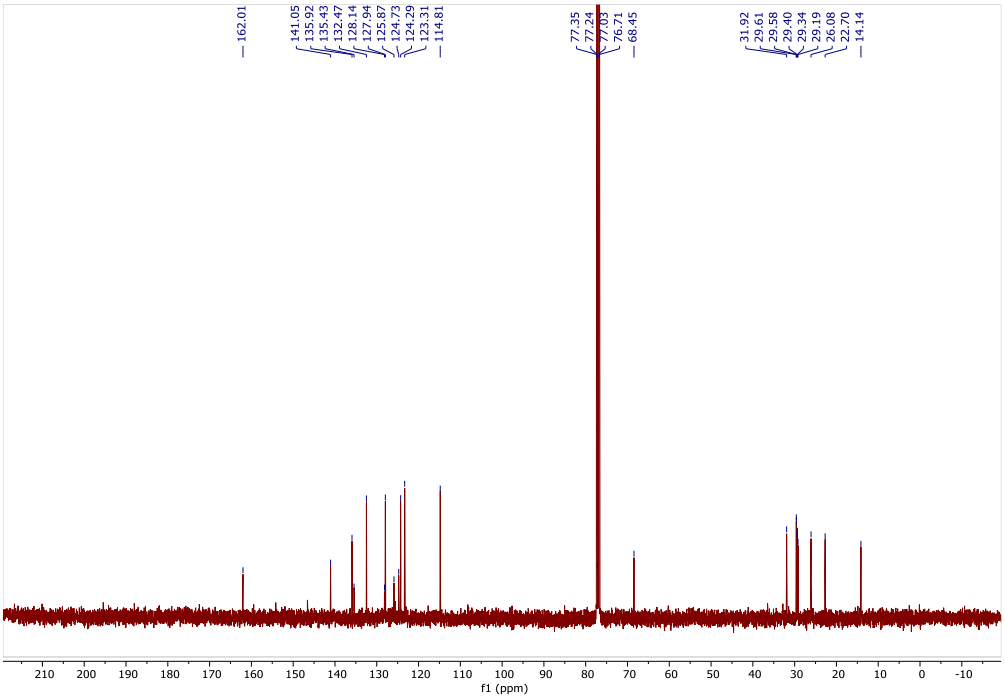

Figure S26. ^{13}C NMR spectrum of **BP-OC$_{10}$ TP2**.

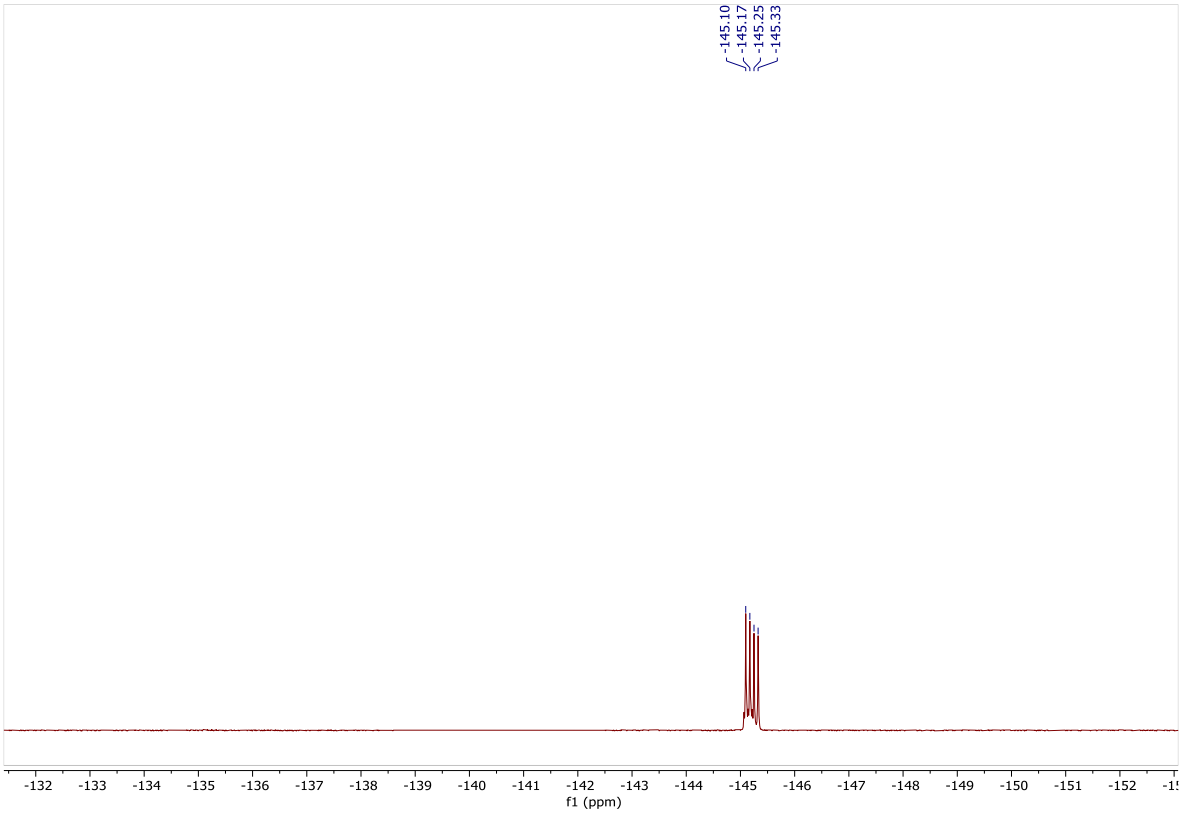

Figure S27. ^{19}F NMR spectrum of **BP-OC$_{10}$ TP2**.

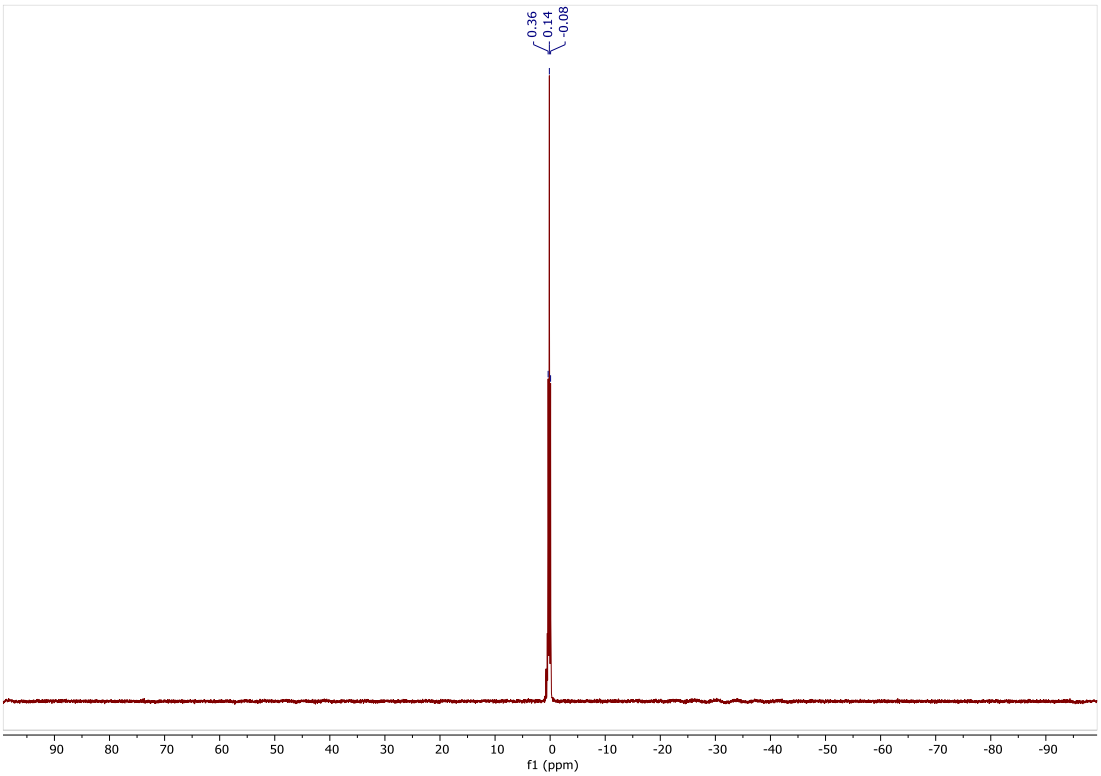

Figure S28. ^{11}B NMR spectrum of **BP-OC$_{10}$ TP2**.

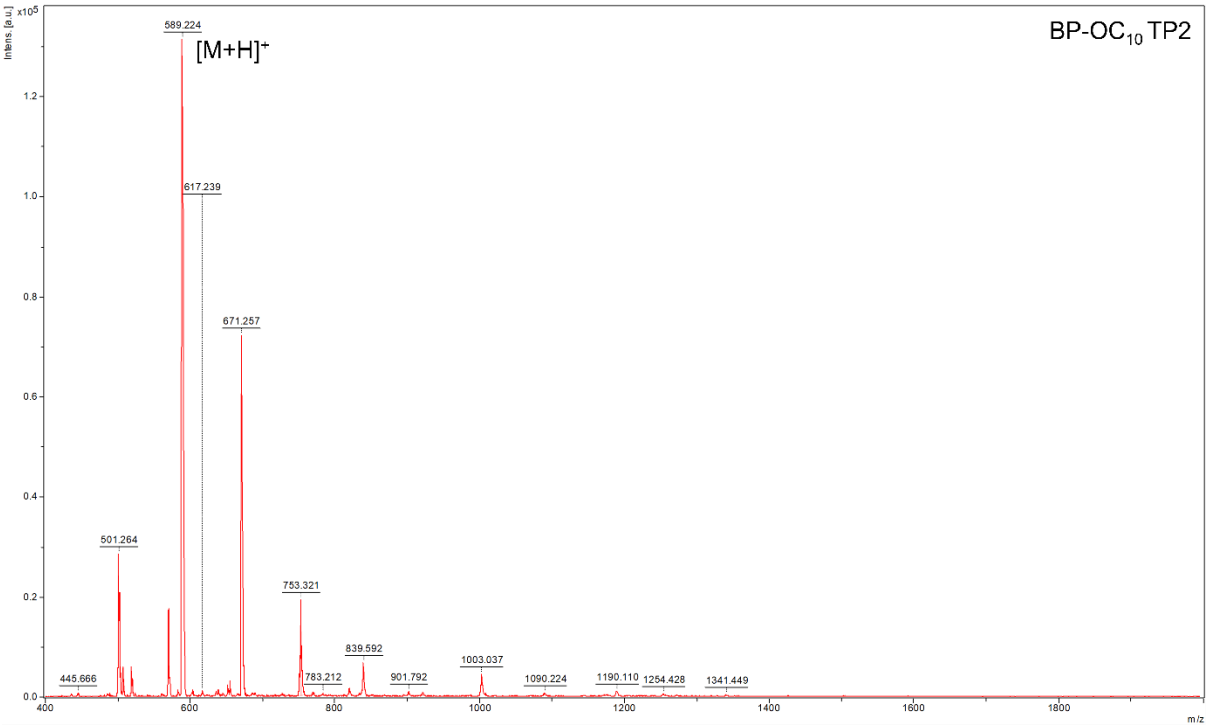

Figure S29. MS spectrum of **BP-OC$_{10}$ TP2.**

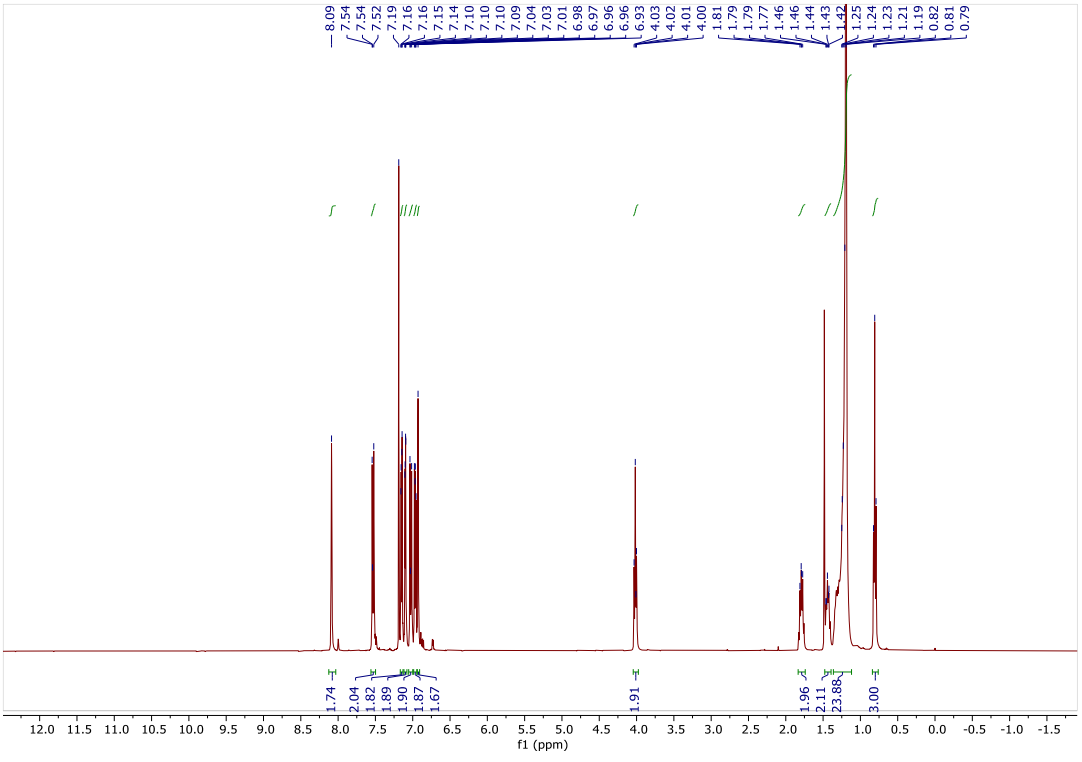

Figure S30. ^{1}H NMR spectrum of **BP-OC$_{16}$ TP2**.

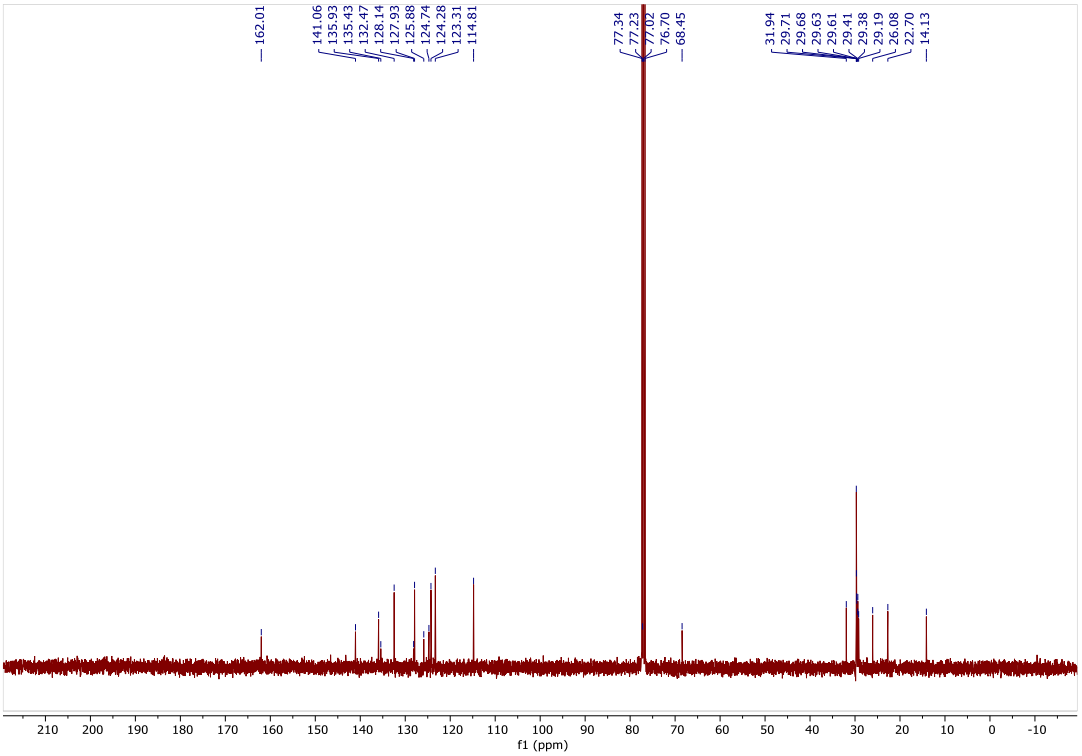

Figure S31. ^{13}C NMR spectrum of **BP-OC$_{16}$ TP2**.

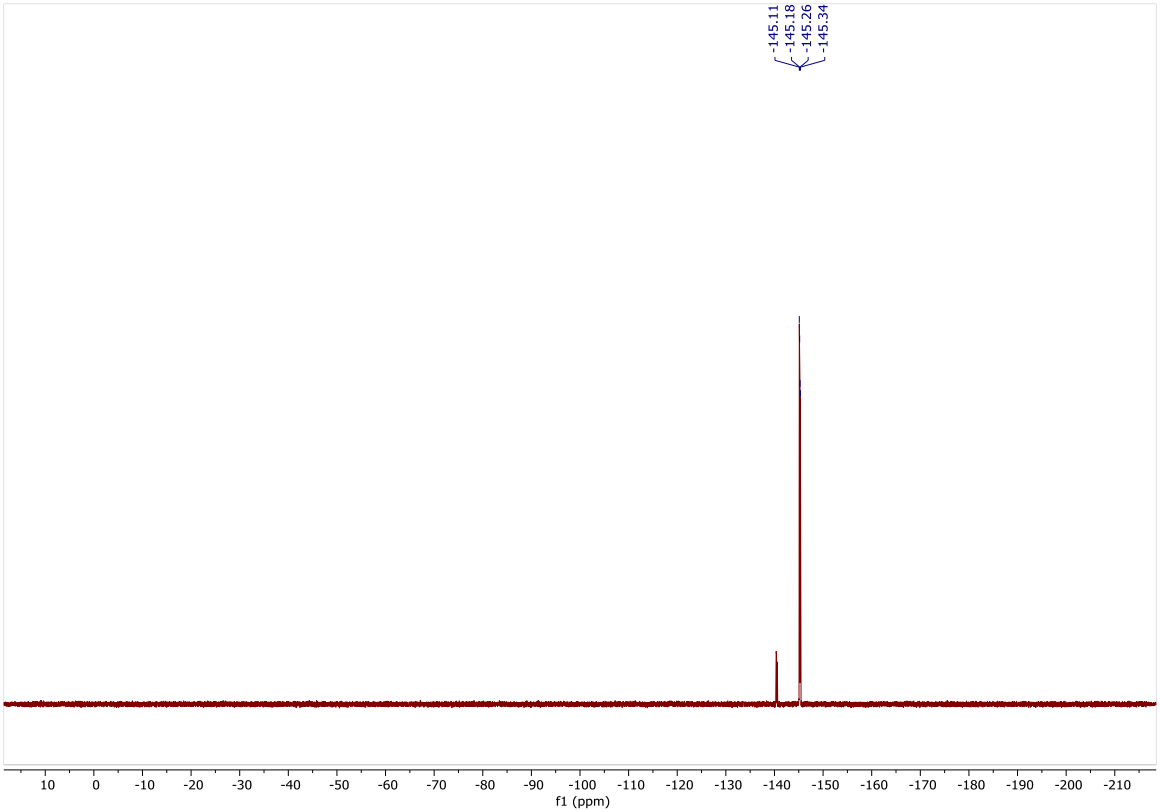

Figure S32. ^{19}F NMR spectrum of **BP-OC$_{16}$ TP2**.

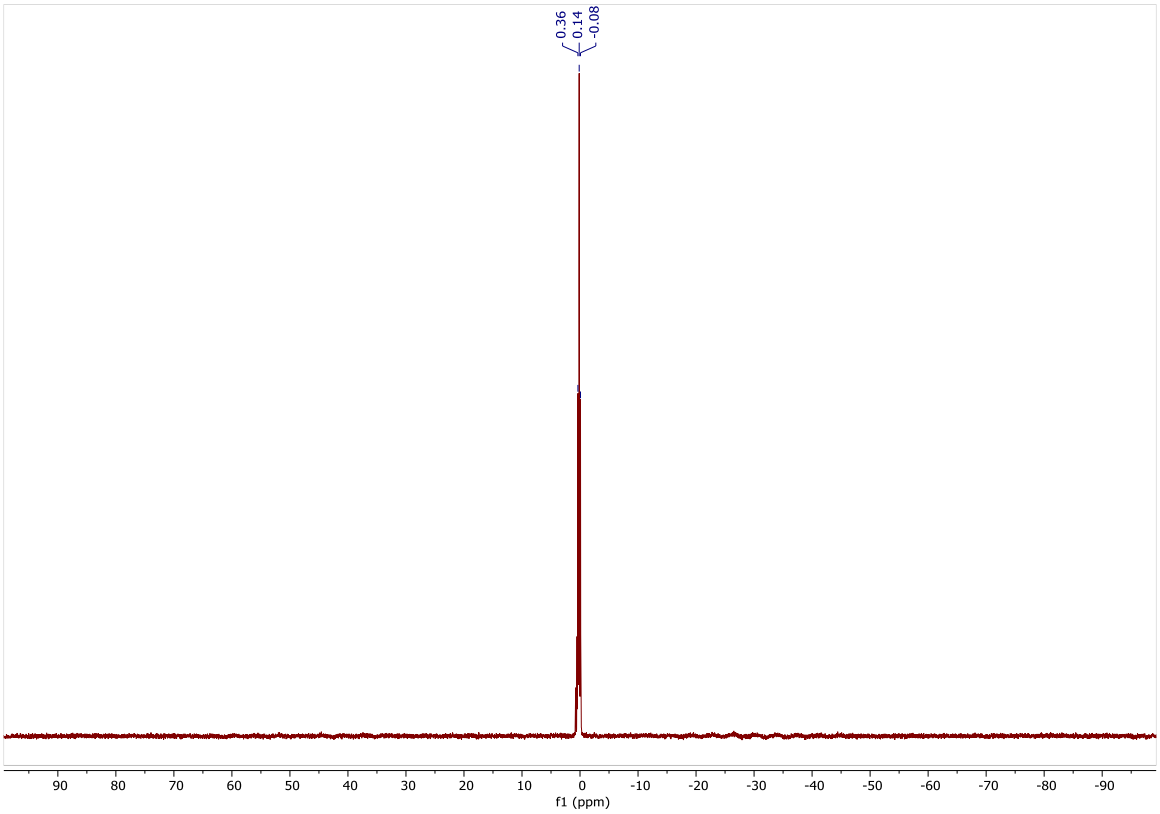

Figure S33. ^{11}B NMR spectrum of **BP-OC$_{16}$ TP2**.

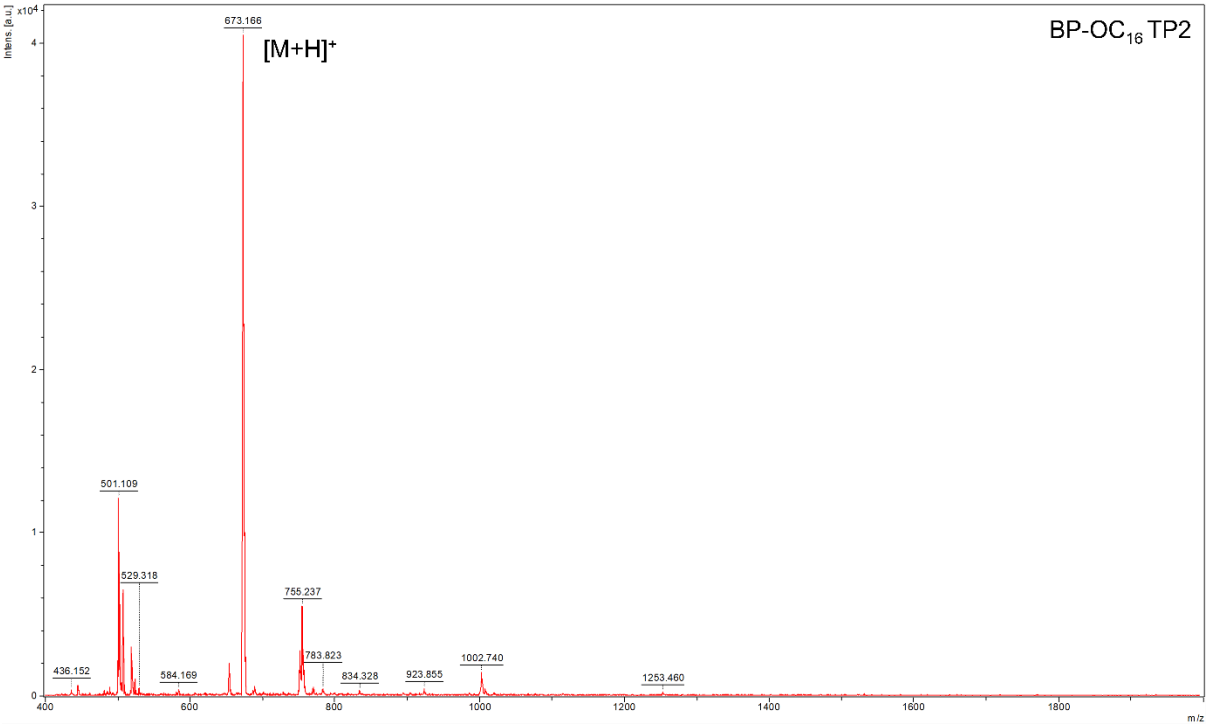

Figure S34. MS spectrum of **BP-OC$_{16}$ TP2.**

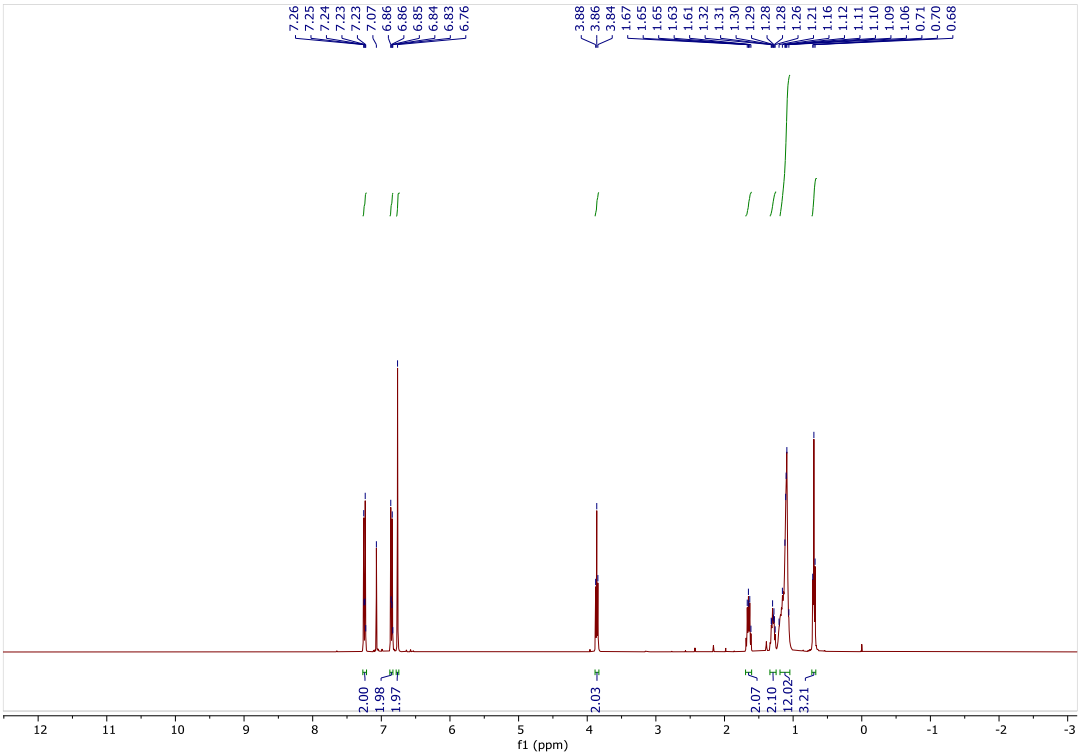

Figure S35. ^{1}H NMR spectrum of **BP-OC$_{10}$ Br4**.

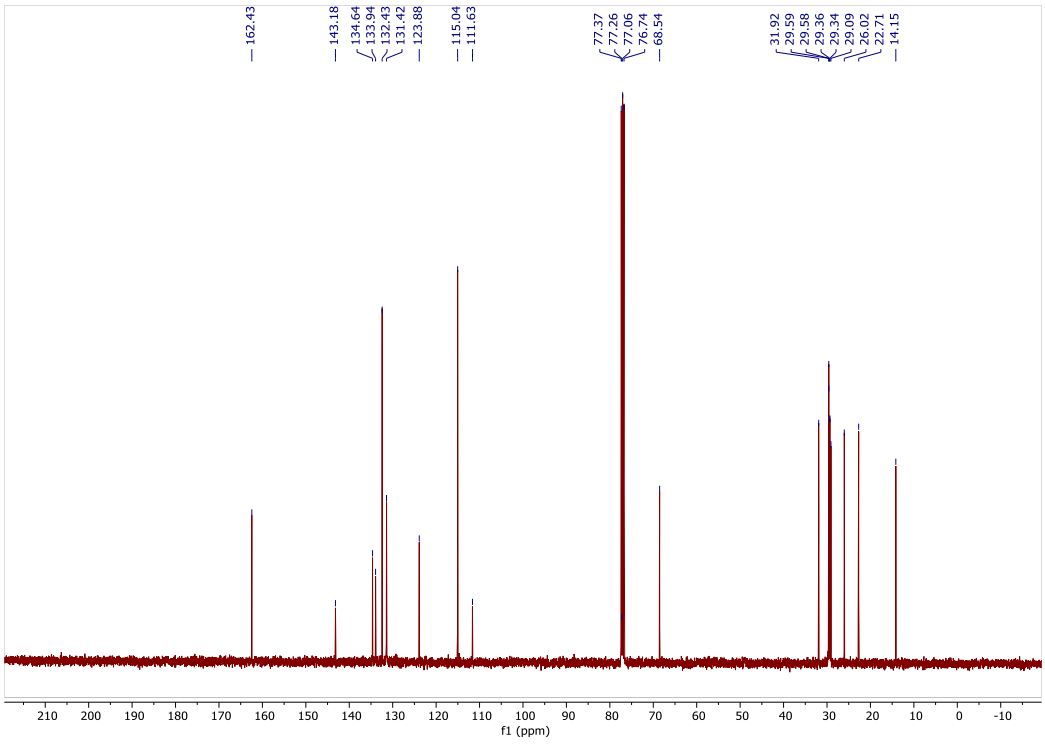

Figure S36. ^{13}C NMR spectrum of **BP-OC$_{10}$ Br4**.

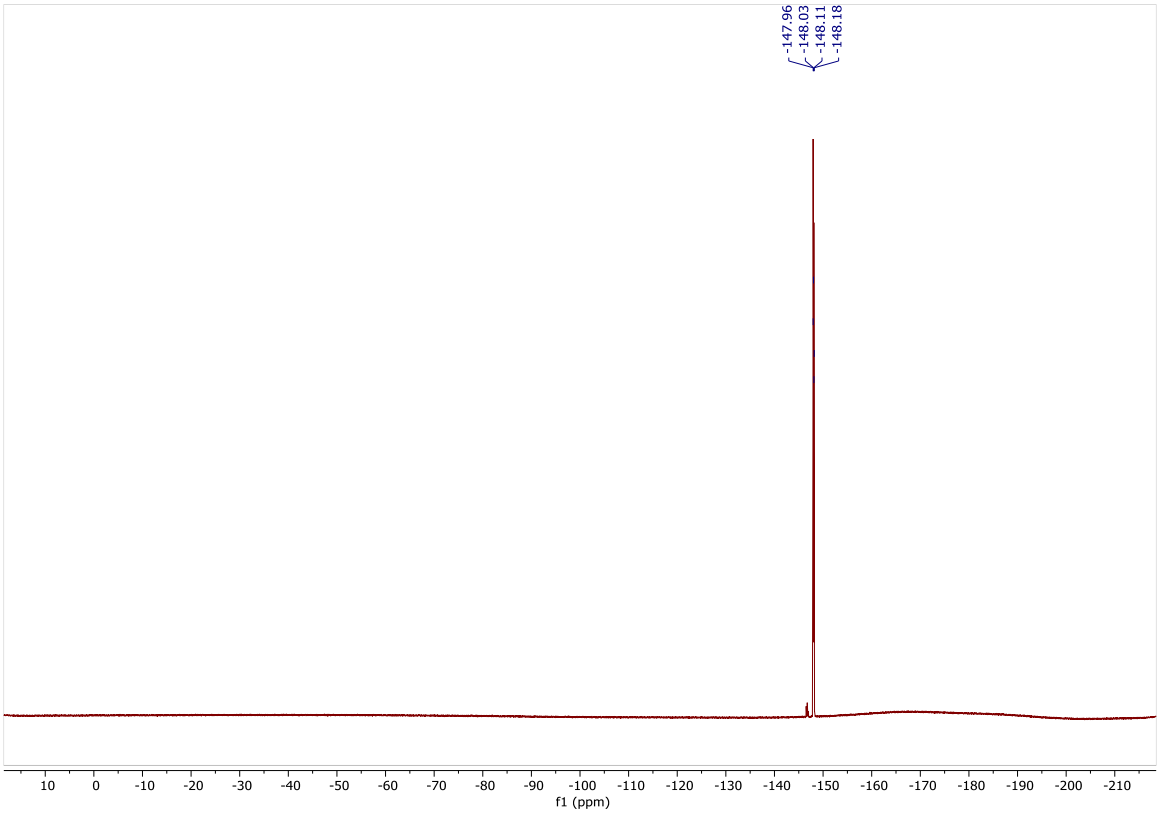

Figure S37. ^{19}F NMR spectrum of **BP-OC$_{10}$ Br4**.

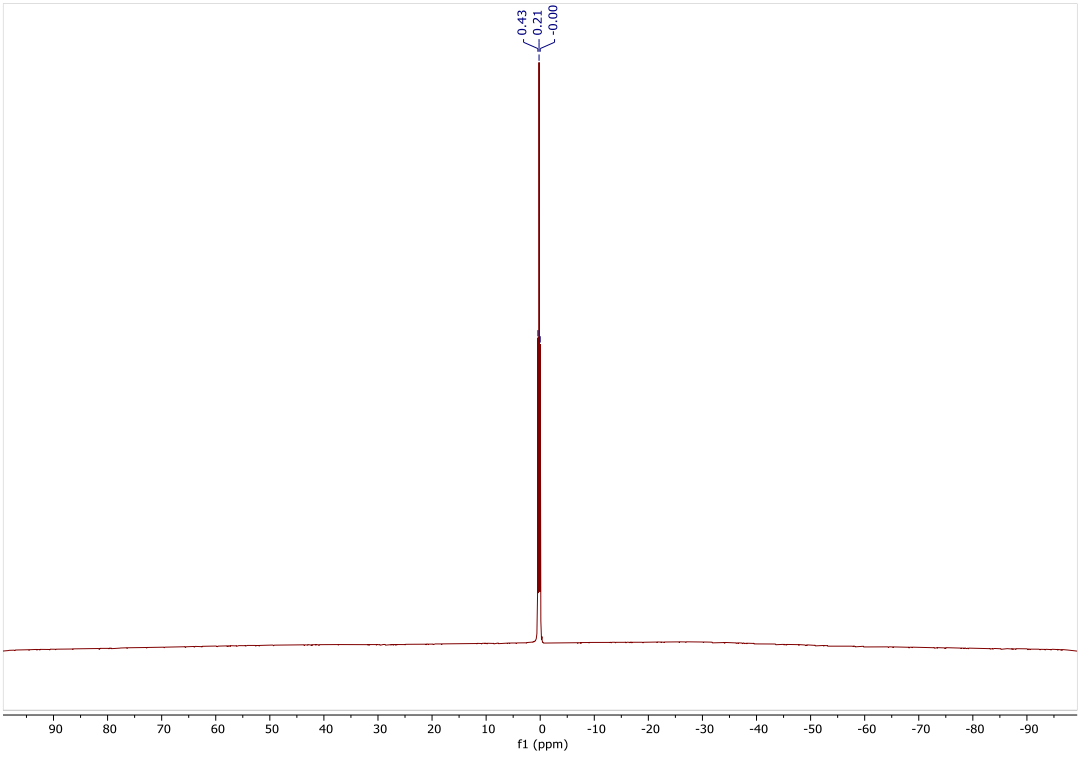

Figure S38. ^{11}B NMR spectrum of **BP-OC$_{10}$ Br4**.

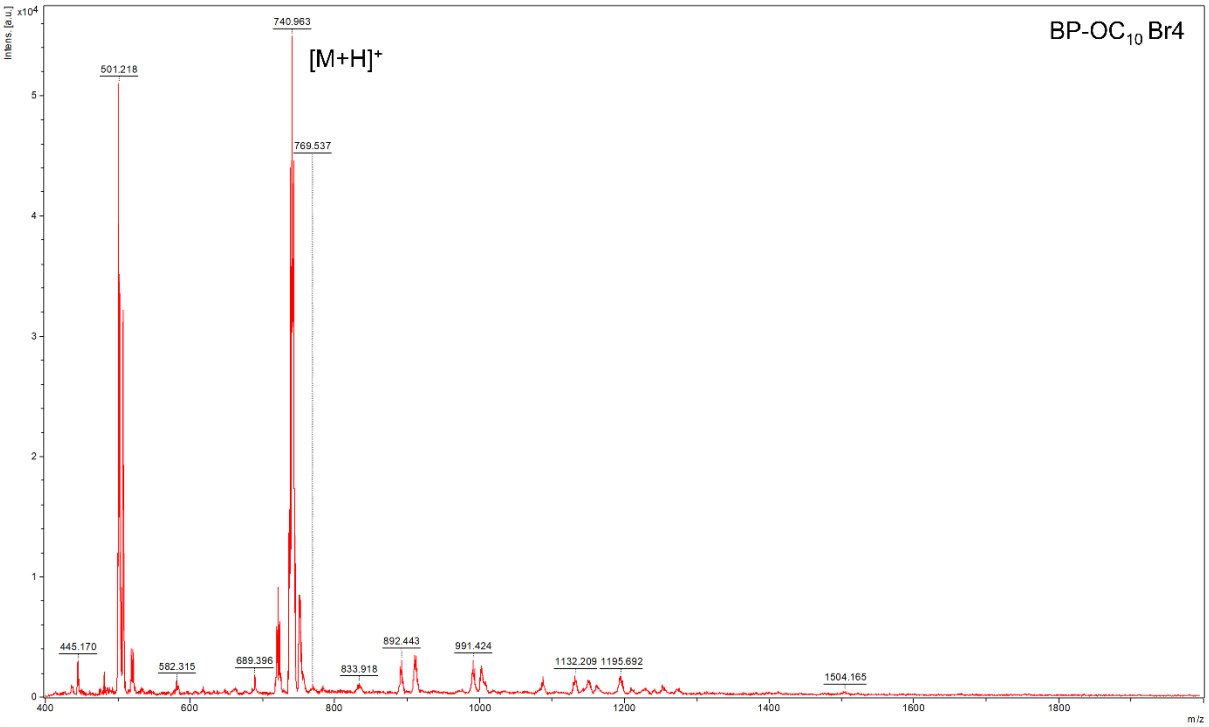

Figure S39. MS spectrum of **BP-OC$_{10}$ Br4.**

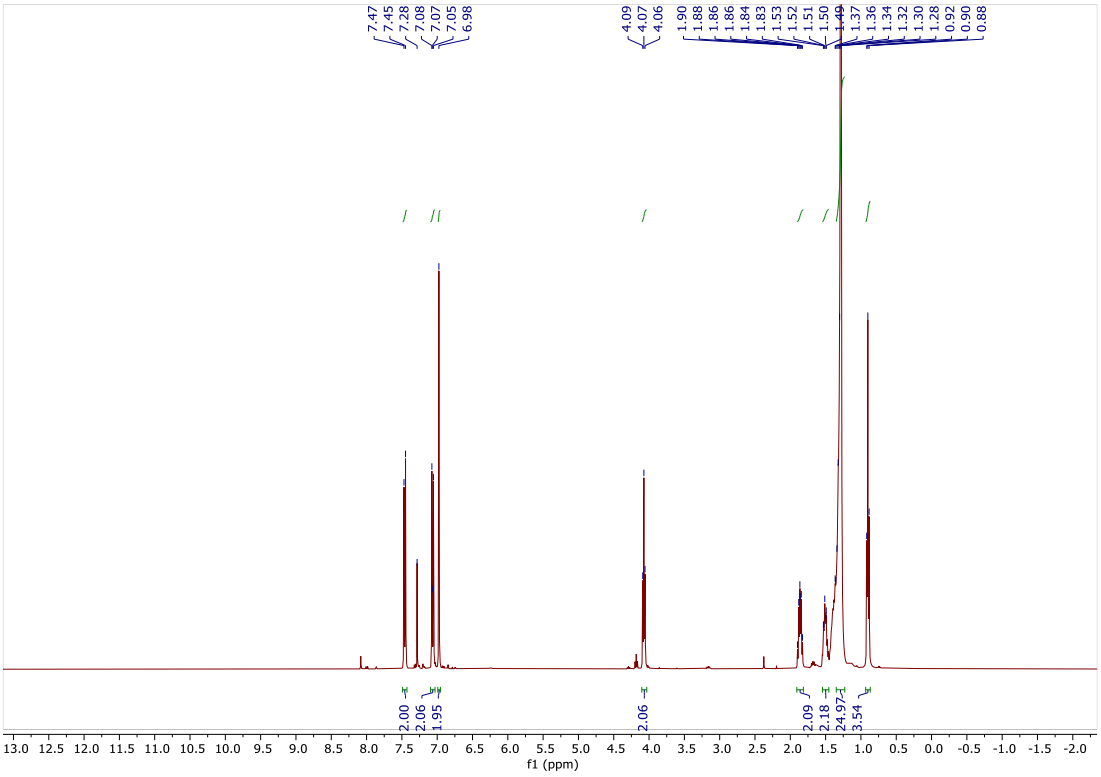

Figure S40. ^{1}H NMR spectrum of **BP-OC$_{16}$ Br4**.

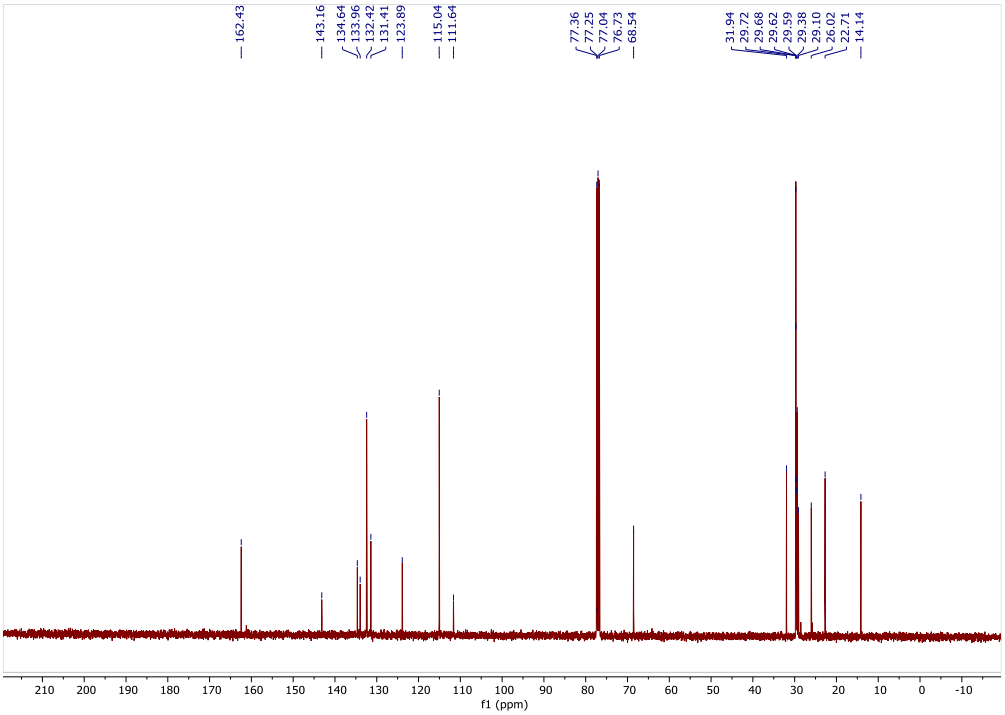

Figure S41. ^{13}C NMR spectrum of **BP-OC$_{16}$ Br4**.

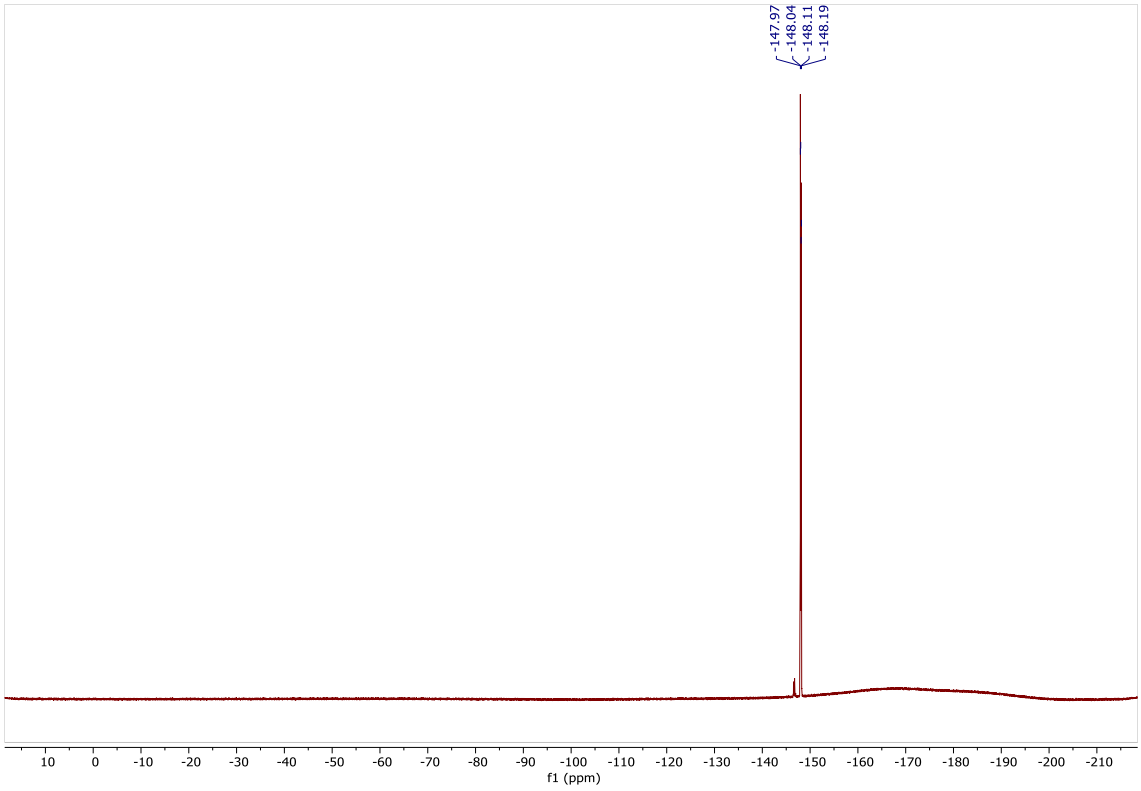

Figure S42. ^{19}F NMR spectrum of **BP-OC$_{16}$ Br4**.

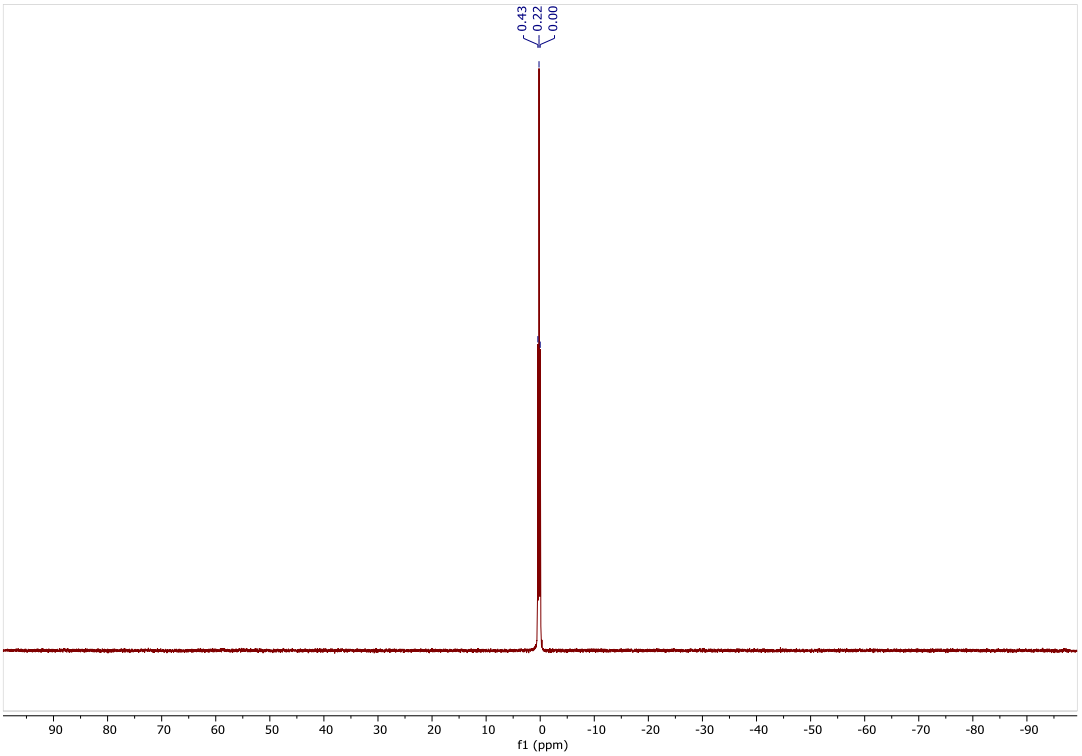

Figure S43. ^{11}B NMR spectrum of **BP-OC$_{16}$ Br4**.

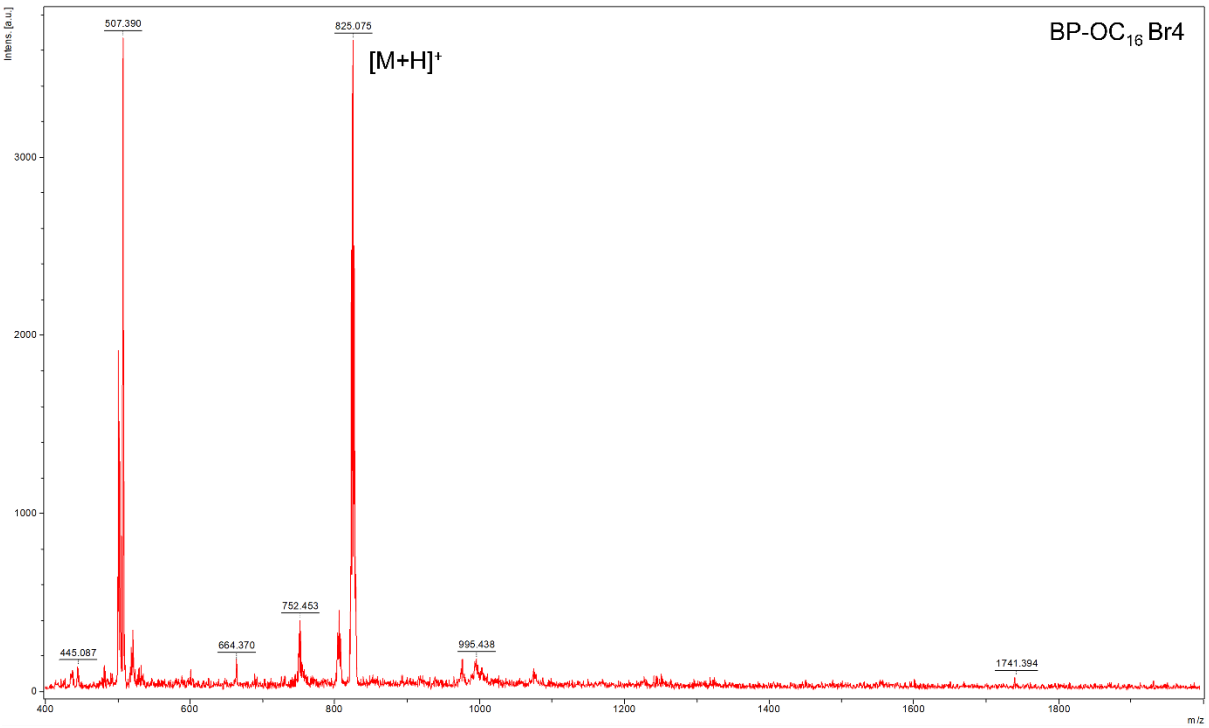

Figure S44. MS spectrum of **BP-OC$_{16}$ Br4.**

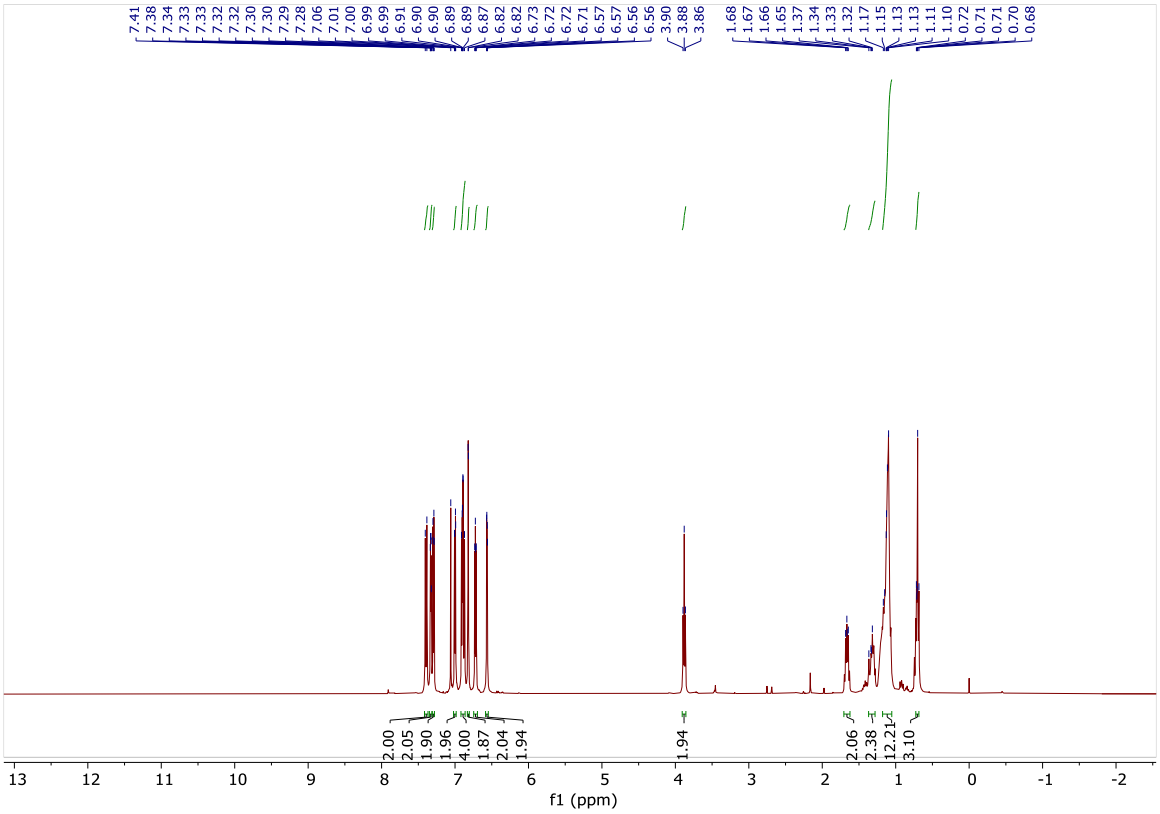

Figure S45. ^{1}H NMR spectrum of **BP-OC$_{10}$ TP4**.

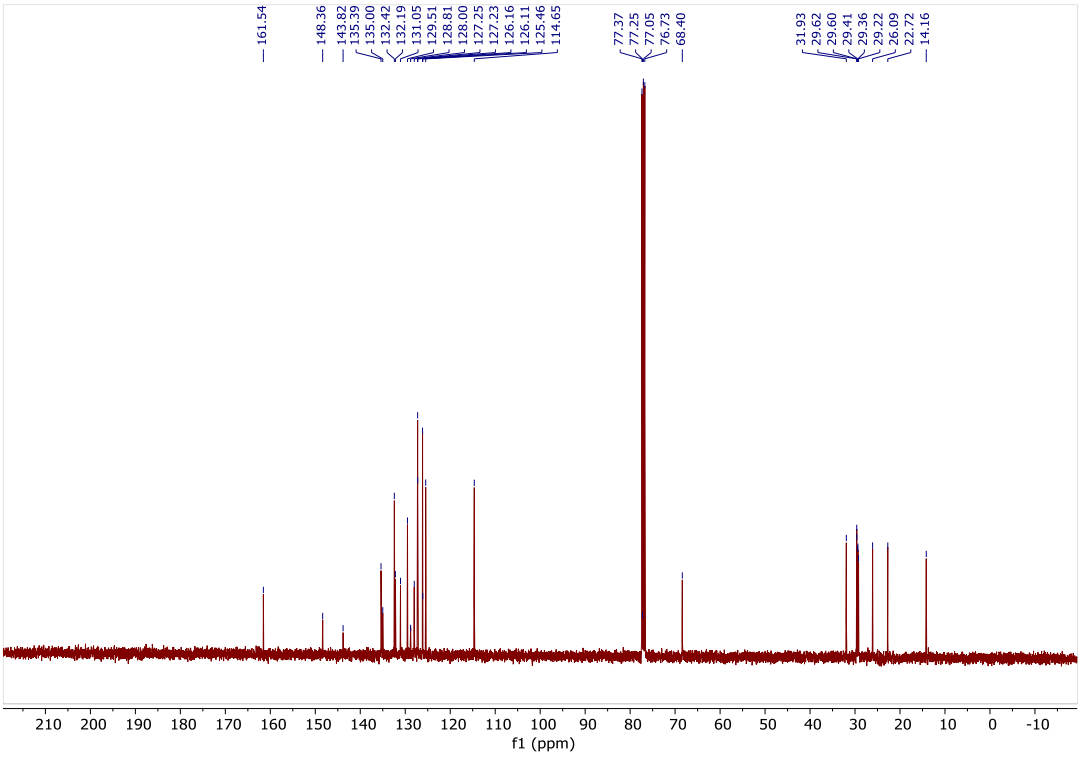

Figure S46. ^{13}C NMR spectrum of **BP-OC$_{10}$ TP4**.

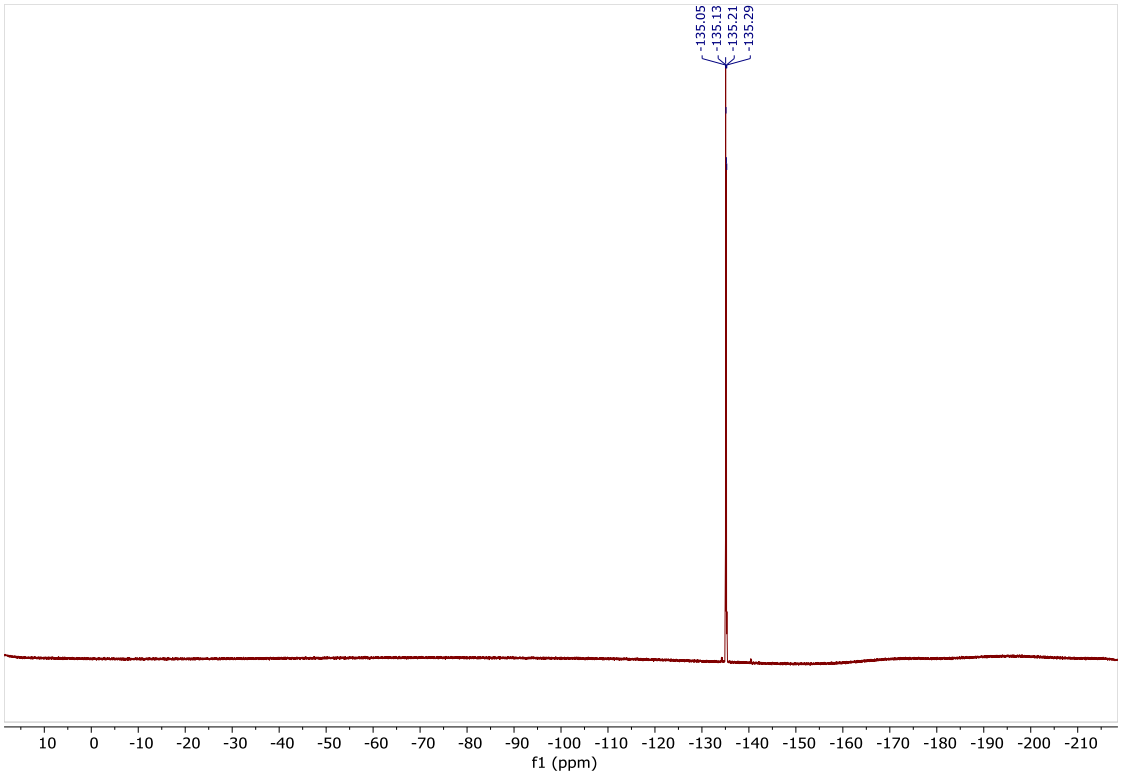

Figure S47. ^{19}F NMR spectrum of **BP-OC$_{10}$ TP4**.

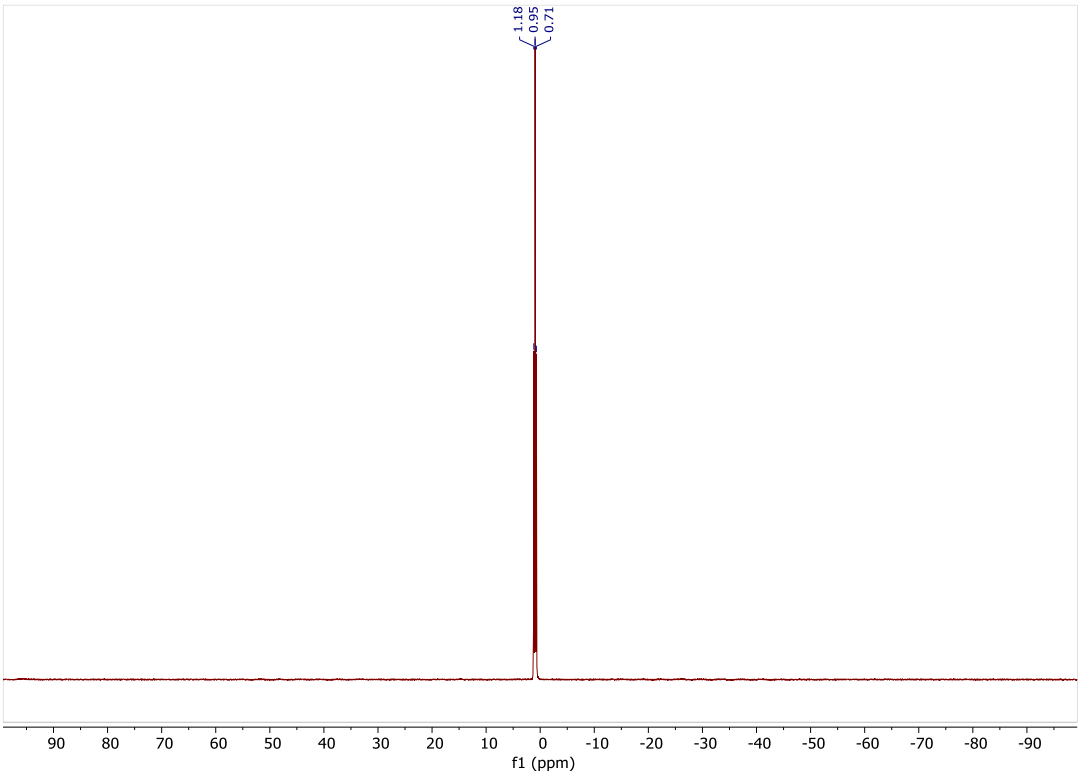

Figure S48. ^{11}B NMR spectrum of **BP-OC$_{10}$ TP4**.

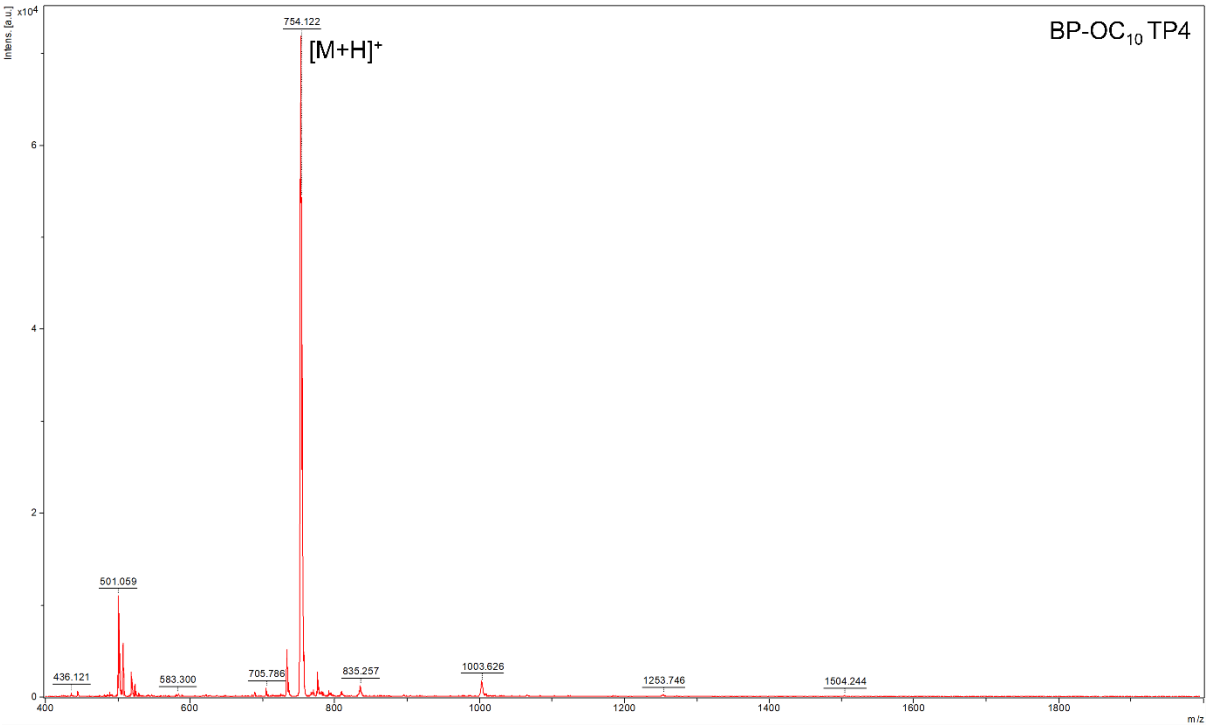

Figure S49. MS spectrum of **BP-OC$_{10}$ TP4.**

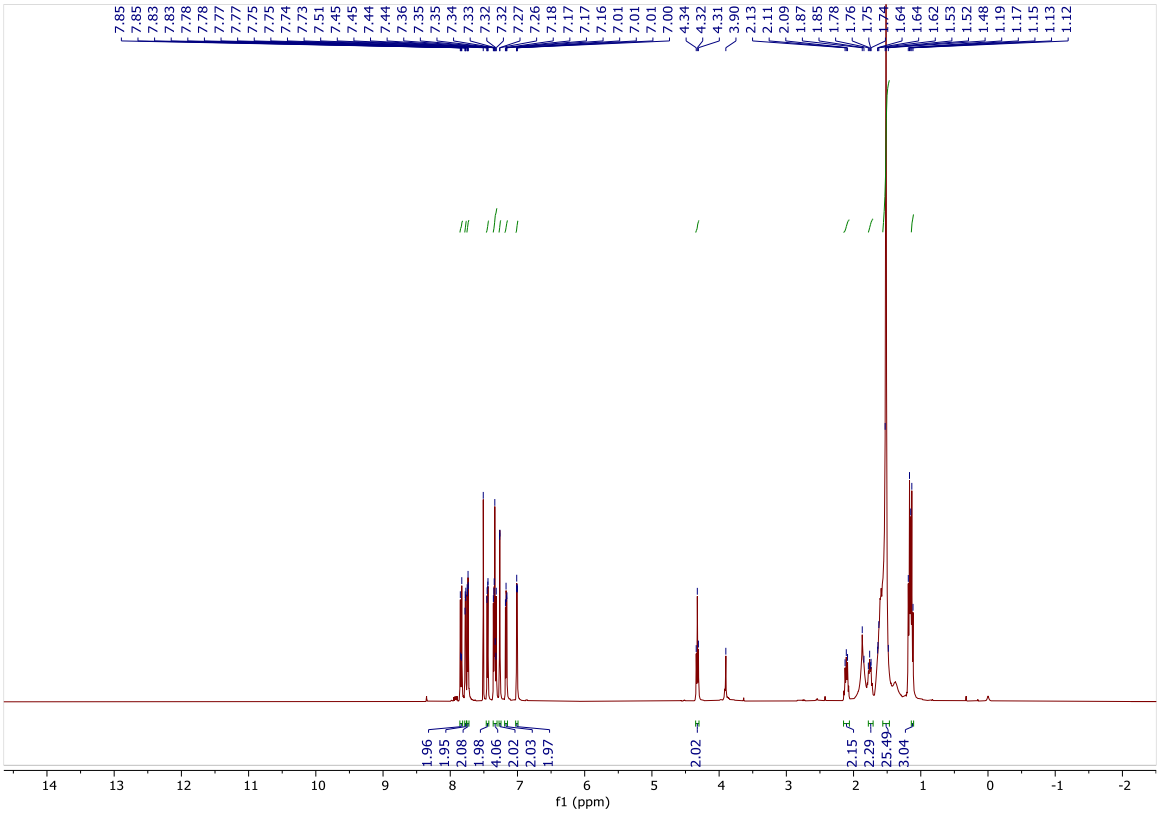

Figure S50. ^{1}H NMR spectrum of **BP-OC$_{16}$ TP4**.

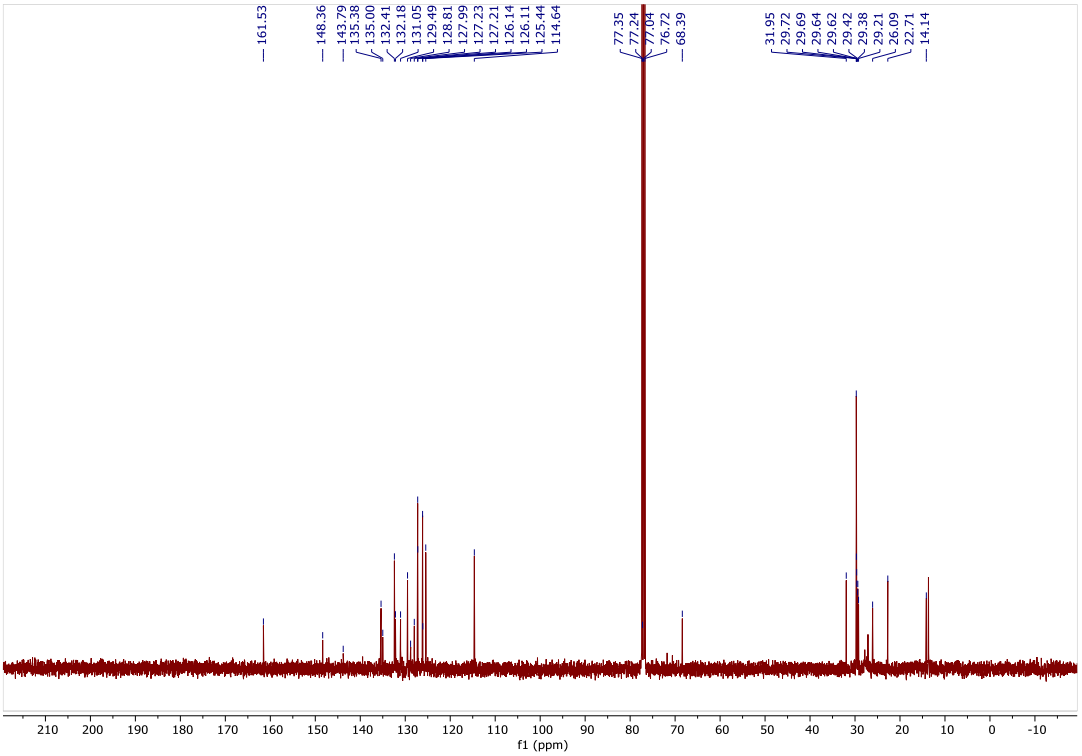

Figure S51. ^{13}C NMR spectrum of **BP-OC$_{16}$ TP4**.

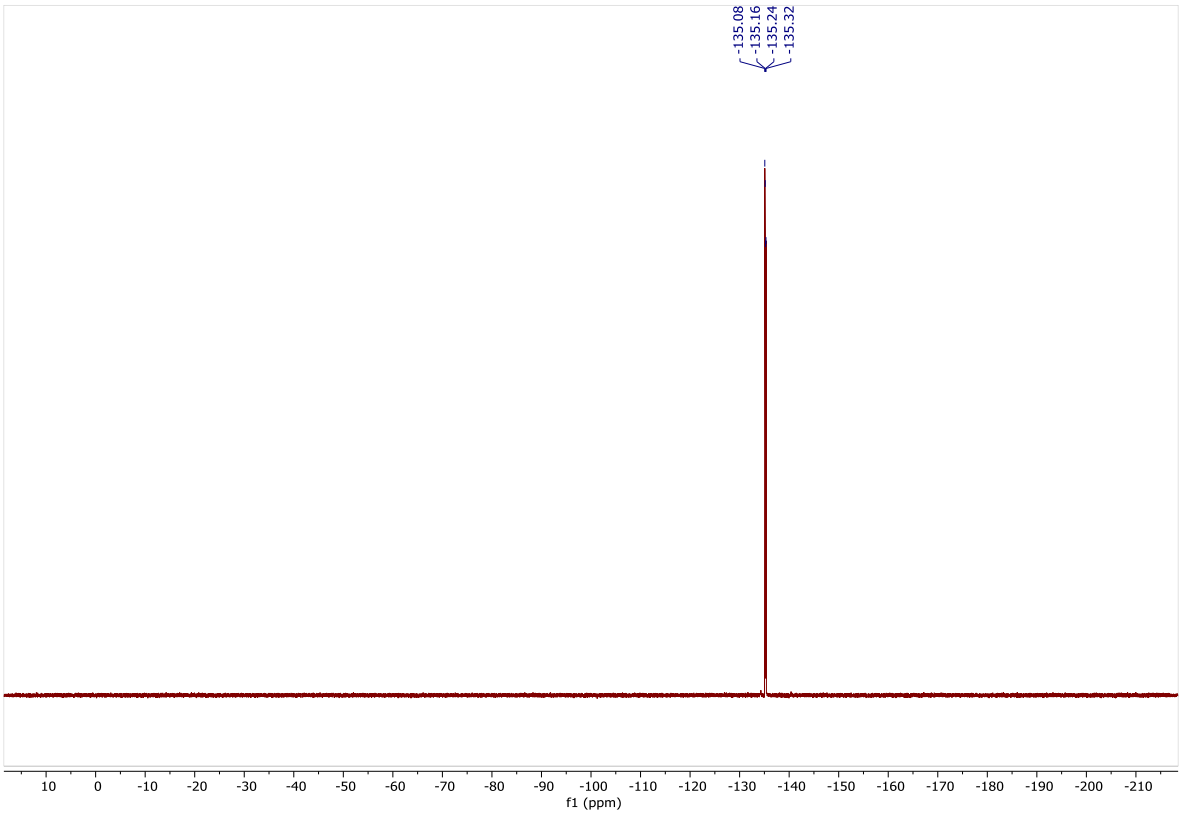

Figure S52. ^{19}F NMR spectrum of **BP-OC$_{16}$ TP4**.

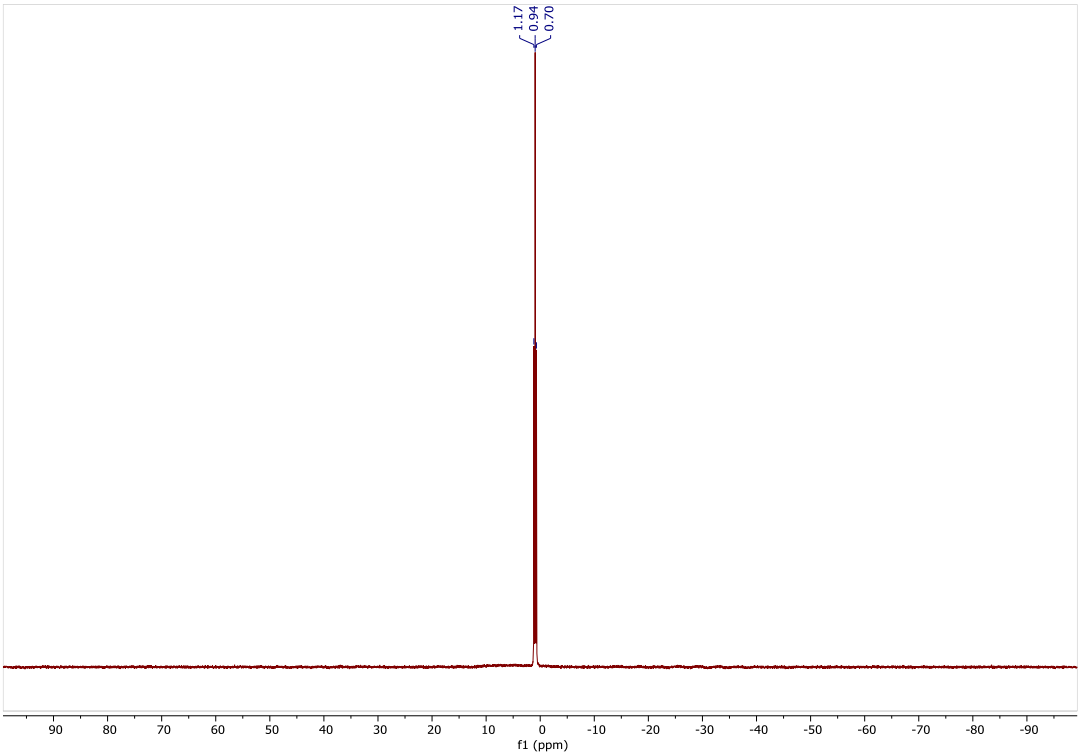

Figure S53. ^{11}B NMR spectrum of **BP-OC$_{16}$ TP4**.

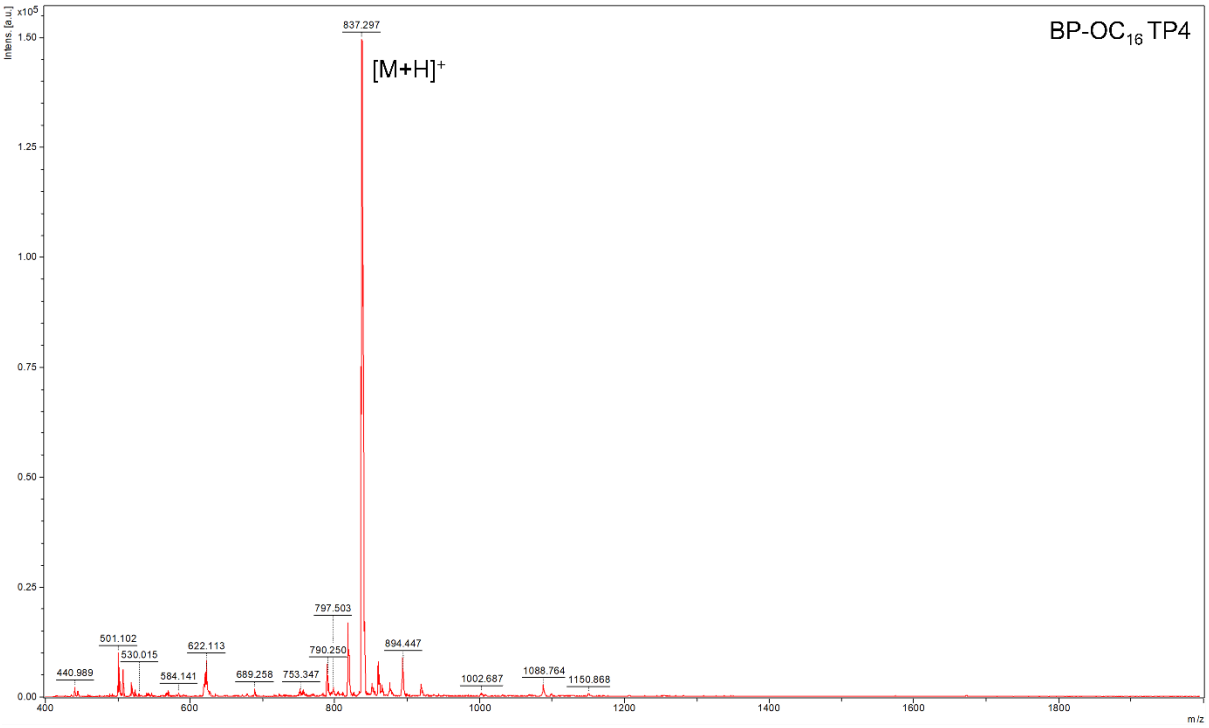

Figure S54. MS spectrum of **BP-OC$_{16}$ TP4.**

4. References

[1] A. Brun, G. Etemad-Moghadam, New Double-Chain and Aromatic (α-Hydroxyalkyl)phosphorus Amphiphiles, *Synthesis,* 2002, **10**, 1385–1390.

[2] T. Nakanishi, N. Miyashita, T. Michinobu, Y. Wakayama, T. Tsuruoka, K. Ariga, D.G. Kurth, Perfectly straight nanowires of fullerenes bearing long alkyl chains on graphite, *Journal of the American Chemical Society*, 2006, **128**, 6328–6329.

[3] R.W. Wagner, J.S. Lindsey, Boron-dipyrromethene dyes for incorporation in synthetic multi-pigment light-harvesting arrays, *Pure and Applied Chemistry*, 1996, **68**, 1373–1380.

[4] M.K. Kuimova, G. Yahioglu, J.A. Levitt, K. Suhling, Molecular rotor measures viscosity of live cells via fluorescence lifetime imaging, *Journal of the American Chemical Society*, 2008, **130,** 6672–6673.

[5] A. Vyšniauskas, I. López-Duarte, N. Duchemin, T.T. Vu, Y. Wu, E.M. Budynina, Y.A. Volkova, E. Peña Cabrera, D.E. Ramírez-Ornelas, M.K. Kuimova, Exploring viscosity, polarity and temperature sensitivity of BODIPY-based molecular rotors, *Physical Chemistry Chemical Physics*, 2017, **19**, 25252–25259.